

## Status and perspectives of CO<sub>2</sub> conversion into fuels and chemicals by catalytic, photocatalytic and electrocatalytic processes†

Cite this: *Energy Environ. Sci.*, 2013, **6**, 3112

Evgenii V. Kondratenko,<sup>\*a</sup> Guido Mul,<sup>b</sup> Jonas Baltrusaitis,<sup>b</sup> Gastón O. Larrazábal<sup>c</sup> and Javier Pérez-Ramírez<sup>\*c</sup>

This review highlights recent developments and future perspectives in carbon dioxide usage for the sustainable production of energy and chemicals and to reduce global warming. We discuss the heterogeneously catalysed hydrogenation, as well as the photocatalytic and electrocatalytic conversion of CO<sub>2</sub> to hydrocarbons or oxygenates. Various sources of hydrogen are also reviewed in terms of their CO<sub>2</sub> neutrality. Technologies have been developed for large-scale CO<sub>2</sub> hydrogenation to methanol or methane. Their industrial application is, however, limited by the high price of renewable hydrogen and the availability of large-volume sources of pure CO<sub>2</sub>. With regard to the direct electrocatalytic reduction of CO<sub>2</sub> to value-added chemicals, substantial advances in electrodes, electrolyte, and reactor design are still required to permit the development of commercial processes. Therefore, in this review particular attention is paid to (i) the design of metal electrodes to improve their performance and (ii) recent developments of alternative approaches such as the application of ionic liquids as electrolytes and of microorganisms as co-catalysts. The most significant improvements both in catalyst and reactor design are needed for the photocatalytic functionalisation of CO<sub>2</sub> to become a viable technology that can help in the usage of CO<sub>2</sub> as a feedstock for the production of energy and chemicals. Apart from technological aspects and catalytic performance, we also discuss fundamental strategies for the rational design of materials for effective transformations of CO<sub>2</sub> to value-added chemicals with the help of H<sub>2</sub>, electricity and/or light.

Received 15th April 2013

Accepted 13th August 2013

DOI: 10.1039/c3ee41272e

[www.rsc.org/ees](http://www.rsc.org/ees)

### Broader context

Preserving the environment for future generations, particularly in light of concerns about climate change linked to anthropogenic CO<sub>2</sub> emissions, is one of the greatest challenges facing today's society. The complexity of this issue is compounded by a myriad of factors, such as the constant push for economic growth, the increase of the world's population and our reliance on fossil fuels. In this context, novel technologies for the sustainable production of energy and chemicals in an economically and environmentally viable manner are urgently needed. One vision for such a technology is using CO<sub>2</sub> as a feedstock for the production of energy carriers and commodity chemicals. This could lessen the amount of CO<sub>2</sub> released into the atmosphere, lead to more sustainable production processes in the chemical industry and unlock valuable synergies with intermittent renewable energy sources. Catalysis plays a fundamental role in all the routes that have been proposed for CO<sub>2</sub> utilisation. This review provides a comprehensive view of the field of CO<sub>2</sub> conversion into fuels and chemicals through heterogeneous catalysis, photocatalysis and electrocatalysis and highlights the technical features, recent advances, current limitations and future perspectives of these routes.

### Setting the CO<sub>2</sub> scene

For the past two centuries, fossil fuels such as natural gas, oil, and coal have been essential for the production of energy and

commodity chemicals. For example, around 90% of the energy produced worldwide in 2011 was derived from fossil fuels. Furthermore, BP's Energy Outlook 2030 predicts that oil will remain the dominant resource of energy for years to come.<sup>1</sup> It is also forecasted that the global energy demand will grow by 36% between 2011 and 2030. Despite the fact that the amount of fossil fuels is finite and resources decrease rapidly due to (i) the development of new processes, (ii) the increased world population, and (iii) a longer life expectancy, they will continue to play a major role in energy generation. This is due to the development of cost effective new technologies, which enable the recovery of oil and gas from *non*-standard sources. For example, 170.4 billion barrels of proven oil reserves are present in the oil sand deposits of Northern Alberta,<sup>2</sup> the world's third largest oil reserve. Certainly,

<sup>a</sup>Leibniz-Institut für Katalyse e.V and der Universität Rostock, Albert-Einstein-Str., 29A, 18059 Rostock, Germany. E-mail: [evgenii.kondratenko@catalysis.de](mailto:evgenii.kondratenko@catalysis.de); Fax: +49-381-128151290; Tel: +49-381-1281290

<sup>b</sup>Photocatalytic Synthesis Group, MESA+ Institute for Nanotechnology, Faculty of Science and Technology, University of Twente, P.O. Box 217, Enschede, NL 7500 AE, The Netherlands

<sup>c</sup>Institute for Chemical and Bioengineering, Department of Chemistry and Applied Biosciences, ETH Zurich, HCI E 125, Wolfgang-Pauli-Strasse 10, Zurich, CH-8093, Switzerland. E-mail: [jpr@chem.ethz.ch](mailto:jpr@chem.ethz.ch); Fax: +41 44 633 1405; Tel: +41 44 633 7120

† Electronic supplementary information (ESI) available: Table S1. See DOI: 10.1039/c3ee41272e

from the point of view of CO<sub>2</sub> emissions, the use of these fossil resources is not sustainable and will further contribute to global warming. Therefore, the environmental and economic incentives to develop processes for the conversion of CO<sub>2</sub> into fuels and chemicals are enormous. For such conversions to become economically feasible, considerable research is urgently required. Another important aspect is the development of CO<sub>2</sub> capture and storage technologies.

According to the report of the Intergovernmental Panel on Climate Change in 2005 (IPCC),<sup>3</sup> around 7900 stationary sources with individual annual CO<sub>2</sub> emissions above 0.1 Mt exist worldwide. Fig. 1 shows a breakdown of the overall annual CO<sub>2</sub> production by selected industry sectors. Fossil-fuel combustion in power stations clearly dominates global CO<sub>2</sub> emissions. Other processes which also contribute to the formation of CO<sub>2</sub> include the production of cement, metals, and bioethanol as well as the refinery and petrochemical industries.

However, the ability to utilise CO<sub>2</sub> strongly depends on the quality of its source, *i.e.* the purity and the partial pressure. In general, the higher the partial pressure, the easier the separation. Fig. 1 shows that the partial pressure of CO<sub>2</sub> in the flue gases of power stations is significantly lower than that in those originating from petrochemical plants (*e.g.*, from the production of ethylene oxide, methanol, hydrogen, and ammonia). As a

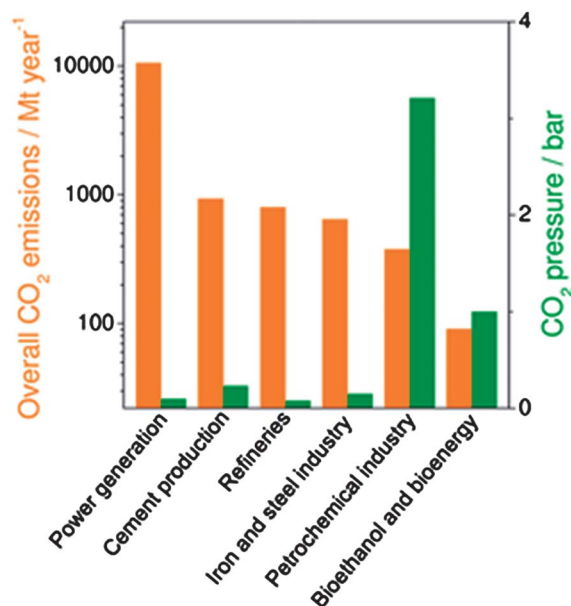


Fig. 1 Total annual CO<sub>2</sub> emissions and partial CO<sub>2</sub> pressures in various industry sectors. Adapted from ref. 3.



*Evgenii V. Kondratenko (Rubtsovsk, Russia, 1967) graduated from the Novosibirsk State University in 1991 (diploma degree in chemistry with specialisation in chemical kinetics). He earned his PhD (Candidate of Chemical Sciences) in 1995 at the Institute of Chemistry of Natural Materials in Krasnoyarsk. In 1997, he was awarded a fellowship from the Alexander von Humboldt Foundation at the*

*Institute for Applied Chemistry Berlin-Adlershof. After a Post-Doc stay at the same institute, he obtained a habilitation degree (the Venia Legendi degree) from the Technical University Berlin in 2007. He is currently working as a group leader ("Reaction Mechanisms") at the Leibniz-Institut für Katalyse e.V. an der Universität Rostock. His research field is functionalisation of C<sub>1</sub>–C<sub>4</sub> alkanes, environmental catalysis, and high-temperature reactions with the focus on mechanistic understanding of catalyst operation and on developing reactor concepts for improved catalyst and/or process design.*



*Guido Mul (1969) obtained his master's degree in chemistry with specialization in heterogeneous catalysis (Prof. Geus) from Utrecht University in 1992. He received his PhD in 1997 from the Delft University of Technology on the in situ DRIFT analysis of catalytic oxidation of (diesel) soot, research conducted under supervision of Prof. Jacob Moulijn. After a Post-Doc position at SRI-International (Stanford Research Institute) in*

*California, USA (1997–1999), he was awarded a fellowship of the KNAW (Royal Netherlands Academy of Arts and Sciences) in 2000. This allowed him to return to Delft University of Technology (TUD) and to determine the detailed mechanism of catalytic oxidation reactions, using an integrated approach based on Infrared and Raman spectroscopies and transient kinetics. In 2005 he was awarded the VIDI grant of the Dutch National Science Foundation (NWO), to initiate fundamental research in the field of photocatalysis. He was appointed associate professor at TU Delft in 2007, with the focus on developing/evaluating spectroscopies (ATR, Raman) for analyses of liquid phase (photo) catalytic processes. He was appointed full professor at the University of Twente in 2009 to conduct research in the field of 'Photocatalytic Synthesis', with research activities in photocatalysis for hydrogen production and CO<sub>2</sub> to fuel conversion, water and air purification, and selective oxidation. Furthermore, development and evaluation of novel reactor concepts based on monoliths and microreactors for (photo) catalysis are part of his current research activities.*

consequence, capturing CO<sub>2</sub> from its largest stationary source, *i.e.* power generation plants, is economically less attractive. When oxy-fuel technology (*i.e.* the combustion of fossil fuels with pure oxygen) is applied, water and pure carbon dioxide are formed. However, this technology is costly as it requires separating oxygen from air. More detailed analysis and description of options for CO<sub>2</sub> recovery from various sources and for its storage are provided in the latest IPCC report.<sup>3</sup>

Once CO<sub>2</sub> is separated, we face the conversion challenge. CO<sub>2</sub> is an awfully stable chemical, which imposes significant energy demands and requires the application of extremely 'talented' catalysts capable of driving its selective conversion into targeted chemicals. CO<sub>2</sub> can be simply incorporated into organic molecules to yield various carbonates, carboxylates, and

carbamates. Such reactions are usually homogeneously catalysed at room temperature. Recent developments in this domain are thoroughly described elsewhere<sup>4,5</sup> and will not be covered herein. It should also be noted that the above approaches are not implemented in large scale and do not provide bulk chemicals and/or fuels. In order to obtain the latter, CO<sub>2</sub> must be chemically reduced, which requires a substantial input of energy. From a sustainable viewpoint, solar light is the ideal energy source. In combination with photocatalytic H<sub>2</sub>O splitting, the solar-driven reduction of CO<sub>2</sub> to fuels is a very attractive approach to reduce CO<sub>2</sub> emissions. Compared to heterogeneous photocatalysts for CO<sub>2</sub> reduction in aqueous solutions, homogeneous ones can be uniformly dispersed thus enabling easier accessibility of dissolved CO<sub>2</sub> to the active sites. However, they are based on expensive metals and need sacrificial reductants. Challenges and developments in this area, specifically related to novel catalytic materials, are discussed in recent authoritative reviews.<sup>6–10</sup> CO<sub>2</sub> dissolved in liquids can also be electrocatalytically converted into hydrocarbons, oxygenates, or carbon monoxide using both heterogeneous and homogeneous systems.<sup>7,11–14</sup> This approach gathers strength when photovoltaic- or wind-derived electricity is used. Another option to directly functionalize CO<sub>2</sub> is its hydrogenation to oxygenates or hydrocarbons *via* modified methanol and Fischer–Tropsch (FT) syntheses.<sup>15–17</sup> Such processes have a greater potential to be applied on a large scale compared to the photo- or electrocatalytic conversion. However, the problem associated with CO<sub>2</sub> hydrogenation is the need for cheap and clean H<sub>2</sub>. Alternatively, CO<sub>2</sub> can react with CH<sub>4</sub> to yield synthesis gas (a mixture of CO and H<sub>2</sub>). The Gas and Metals National Corporation in Japan has successfully performed pilot plant tests for the production of liquid fuels from synthesis gas obtained *via* a combined CO<sub>2</sub> and H<sub>2</sub>O reforming of natural gas followed by FT synthesis.<sup>18</sup>

Compared with available accounts on specific CO<sub>2</sub> transformations, this review discusses recent developments in CO<sub>2</sub> technologies *via* the catalytic hydrogenation as well as electro- and photocatalytic approaches for the production of



*Jonas Baltrusaitis was born in June 24, 1976 in Marijampole, Lithuania. He graduated from Kaunas University of Technology, Lithuania with BSc and MSc degrees in Chemical Engineering in 1998 and 2000, and then worked in the chemical industry as a process engineer. In 2003 he was accepted to the University of Iowa, Department of Chemistry where he graduated in 2007 with a PhD in Physical Chemistry.*

*During his graduate career, he worked in Prof. Vicki Grassian's group on the atmospheric and environmental chemistry topics, surface chemistry, microscopy and spectroscopy. After his PhD and post-doc, JB worked in Central Microscopy Research Facility at the University of Iowa as a research scientist. In 2012, JB has become an assistant professor in the Photocatalytic Synthesis Group, University of Twente, the Netherlands. His research is now at the nexus between energy and environment in designing low key, sustainable methods and materials for energy conversion. JB has been happily married to his wife Marija for 10 years and is a proud owner of 2 adopted dogs.*



*Gastón O. Larrazábal (Caracas, Venezuela, 1987) earned his BS degree in Chemical Engineering from Universidad Simón Bolívar (2010) and his MSc degree in Process Engineering (2013) from ETH Zurich. He has recently started his PhD studies at ETH Zurich under the supervision of Prof. Javier Pérez-Ramírez. Gastón is interested in the development of electrocatalytical processes for the conversion of carbon dioxide into fuels and chemicals.*



*Javier Pérez-Ramírez (Benidorm, Spain, 1974) studied Chemical Engineering at the University of Alicante, Spain and earned his PhD degree at TU Delft, Netherlands in 2002. After a period in industry he was appointed ICREA research professor at ICIQ in Tarragona, Spain. In 2010, he took the chair of Catalysis Engineering at the Institute for Chemical and Bioengineering of the ETH Zurich.*

*He is engaged in the development and understanding of new heterogeneous catalysts, multifunctional materials, and reactor engineering concepts devoted to sustainable technologies.*

higher-value chemicals with the aim of identifying unifying guidelines for the improvement of these processes. Since our expertise lies in heterogeneous catalysis, the emphasis will be on heterogeneous transformations. We will also elaborate on the possibilities for integrating different technological approaches.

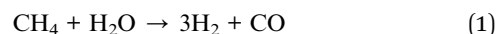
## Catalytic hydrogenation of CO<sub>2</sub>

### Key issue: H<sub>2</sub> sources

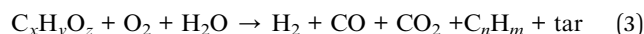
Since molecular hydrogen does not naturally exist in its pure form, it is typically derived from natural gas, oil, coal, biomass, and water by means of various chemical, physico-chemical, photolytic, electrolytic or biological transformations. From an environmental viewpoint, it is crucial that its production is also CO<sub>2</sub> emission free. Since hydrogen can actually substitute fossil fuels, it opens the possibility to even have a positive CO<sub>2</sub> balance, *i.e.* reducing overall CO<sub>2</sub> production, when generating heat and energy upon hydrogen combustion yielding H<sub>2</sub>O as the only product. Fig. 2 shows possible H<sub>2</sub> production routes with the corresponding energy sources. As this contribution is not aimed at reviewing developments in this research area, we will only briefly describe commercially available and prospective approaches. The emphasis will be on their environmental impact and economy in CO<sub>2</sub> hydrogenation to value-added chemicals. Detailed information on various aspects of hydrogen production can be found elsewhere.<sup>19–24</sup>

Steam reforming of methane (eqn (1)) is the main source of hydrogen today.<sup>25</sup> Since this reaction also results in CO, the latter is oxidised to non-toxic CO<sub>2</sub> through the water-gas shift reaction in a separate reactor with simultaneous generation of molecular hydrogen (eqn (2)). Moreover, the steam reforming of methane is energy intensive due to its high endothermicity. This energy is presently generated by the combustion of fossil fuels which also simultaneously produces carbon dioxide. The latter emissions are minimised when steam reforming is performed in the presence of gaseous oxygen (autothermal reforming). Even though these reactions are well optimised,

there are economic needs for their further improvements with respect to the catalyst activity, ratio of H<sub>2</sub> : CO, resistance to deactivation *via* coking and poisoning by sulphur compounds.<sup>26</sup> Furthermore, cost-effective and eco-efficient technologies for air separation are required for autothermal reforming.



Biomass can also be directly converted to hydrogen through liquefaction, pyrolysis, and gasification.<sup>22,27</sup> The latter seems to be the most attractive, because it can profit from existing commercially applied coal gasification technologies. Gasification occurs above 1000 K in the presence of oxygen and/or water (eqn (3)). This conversion process results in a mixture of H<sub>2</sub>, CO, CO<sub>2</sub>, CH<sub>4</sub> and other gas-phase, liquid or solid carbon-containing by-products. Taking into account the renewable nature of biomass, such hydrogen production can be considered to be CO<sub>2</sub>-neutral. When combining the biomass gasification with coal gasification, which seriously suffers from significant amounts of co-produced CO<sub>2</sub>, the environmental impact of the latter process can be minimised. Hydrogen can also be produced through reforming reactions of bio-liquids such as ethanol, glycerol, sugars, or bio-oils.<sup>22</sup> According to the Hydrogen Production Roadmap,<sup>23</sup> the development of commercial technologies for biomass gasification can be completed by 2017, since a common drawback with such conversions is catalyst deactivation due to coking and sulphur poisoning. Another important need is for cheap technologies for the capture and storage of high amounts of CO<sub>2</sub> and solid carbon deposits formed as by-products. In addition, any biomass-based routes to produce hydrogen suffer from unpredictable feedstock quality, regional and seasonal dependency, and finally high operation and maintenance costs. Therefore, further improvements in hydrogen production *via* biomass gasification are expected to be achieved through the development of sulphur- and carbon-tolerant catalysts and separation technologies.



Water electrolysis is industrially applied to produce oxygen and high-purity hydrogen (eqn (4)), eliminating expensive separation costs. Available commercial low-temperature electrolyzers operate with efficiencies between 50 and 70%.<sup>27</sup> Electricity production is the dominant cost, and also contributes to air pollution due to the formation of CO<sub>2</sub>, when generated from fossil fuels. When electricity produced with the help of wind or sunlight is applied, the formation of molecular hydrogen through water electrolysis is free from carbon dioxide emissions. However, the suitability of both wind and solar energy is climate and therefore geographically dependent. Consequently, major challenges are to ensure resourceful operation over a wide range of weather conditions, as well as quick and safe response to their changes.

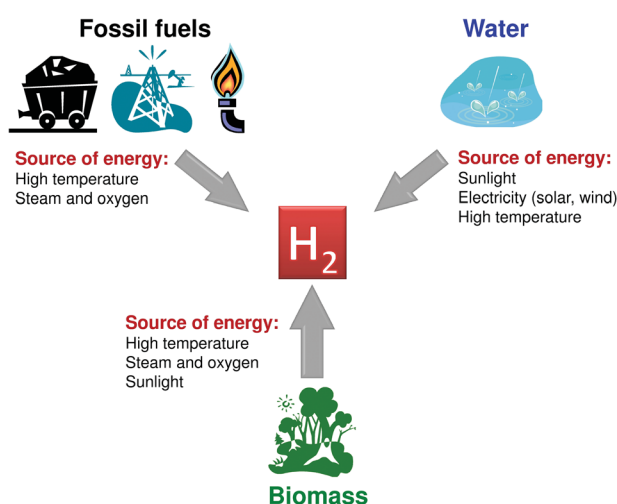


Fig. 2 Primary materials and energy sources for H<sub>2</sub> generation.

Water can also be split into hydrogen and oxygen using sunlight and a photocatalyst. Typically, oxides, nitrides or sulphides of metals with  $d^0$ ,  $d^{10}$ , and  $f^0$  electronic configurations show catalytic activity for the target reaction.<sup>28–31</sup> The role of such catalysts can also be fulfilled by some biological microorganisms, like green algae or cyanobacteria.<sup>32</sup> Both ways of hydrogen production are very attractive, but are still far from a possible industrial application due to the low productivity. Several developments are needed to produce hydrogen from water on an industrial level by photocatalysis. According to ref. 21 and 23, catalytic materials are required, which (i) provide a solar-to-hydrogen efficiency higher than 16% and (ii) are stable against oxidation and (iii) can produce hydrogen for longer than 15 000 hours.

In summary, water is concluded to be the only suitable source of hydrogen for reducing  $\text{CO}_2$  emissions from various sources *via* its hydrogenation to valued-added chemicals. This is due to the fact that  $\text{H}_2$  and  $\text{O}_2$  are the only reaction products of water splitting, meaning that  $\text{CO}_2$  emissions can be avoided when using a  $\text{CO}_2$  free energy source. In contrast, hydrogen generation from fossil fuels and biomass leads to the co-production of  $\text{CO}_2$  and  $\text{CO}$  (eqn (1) and (3)). Therefore,  $\text{CO}_2$  neutrality can only be realized if the cogenerated  $\text{CO}_2$  is hydrogenated in subsequent process steps, rather than consuming/treating  $\text{CO}_2$  originating from other sources.

### $\text{CO}_2$ hydrogenation by heterogeneous catalysts

Hydrogen and methane are two high-energy materials, which can be used for the large-scale transformation of carbon dioxide to valuable products. Fig. 3 illustrates the most attractive heterogeneously catalysed routes. It is important to highlight that the  $\text{H}_2$ -based routes directly yield fuels or chemical building blocks, while the  $\text{CO}_2$  conversion with  $\text{CH}_4$  results in syngas, which can be converted to the above products in an additional process step. From an economic point of view, the direct transformation of  $\text{CO}_2$  is preferable.

### Conversion of $\text{CO}_2$ to hydrocarbons

The hydrogenation of  $\text{CO}_2$  to  $\text{CH}_4$  is highly important from an industrial viewpoint. There are several uses of methane within

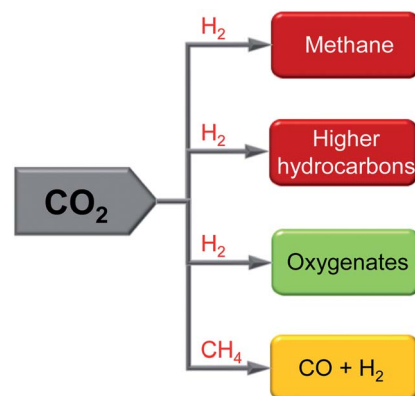


Fig. 3  $\text{CO}_2$  conversions to fuels or useful commodity chemicals.

the existing commercial infrastructure: (i) for the steam reforming of methane to syngas, (ii) for heat and electricity generation, and (iii) as a substitute for gasoline, diesel or liquid petroleum gas in vehicles. The importance of the latter application is illustrated by the “e-gas project” initiated by Audi AG in 2011 in Hamburg.<sup>33</sup> Together with regional energy suppliers in Northern Germany, Audi AG participates in building wind mills at an offshore park in the North Sea. The wind-generated energy will be applied for water electrolysis to obtain hydrogen and oxygen (eqn (4)). Hydrogen produced in this way is applied for the conversion of  $\text{CO}_2$  from bio-gas to  $\text{CH}_4$ . The planned annual production of 1 kt of  $\text{CH}_4$  would translate to the conversion of 2.8 kt of  $\text{CO}_2$ . The resulting  $\text{CH}_4$  can be used for vehicles and also transported to other regions in Europe through the existing natural gas transportation system. Thus, the methanation of  $\text{CO}_2$  opens the possibility of producing  $\text{CH}_4$  in places where  $\text{H}_2$  is generated using renewable energy sources and thereafter to use it everywhere.

Supported noble metals or nickel catalyse the methanation of  $\text{CO}_2$ . Catalysts, reaction conditions, and mechanistic concepts are thoroughly reviewed by Wang *et al.*,<sup>34</sup> covering the literature up to 2010. Among the metals tested, Ru exhibits superior activity and selectivity (Table 1). Since the conversion of  $\text{CO}_2$  to  $\text{CH}_4$  is exothermic, it is highly desired to develop catalysts for low temperature operation favouring high degrees of  $\text{CO}_2$  conversion. Low temperatures are also favourable for suppressing the undesired reverse water-gas shift (RWGS) reaction, which is endothermic. Abe *et al.*<sup>35</sup> reported 100% yield of  $\text{CH}_4$  at 453 K on a Ru/ $\text{TiO}_2$ -anatase catalyst. This catalyst did not lose its activity over at least 170 h on-stream. It was also active even at room temperature with a reaction rate of  $40 \text{ nmol CH}_4 \text{ min}^{-1} \text{ g}^{-1}$ . It was concluded that the size of Ru nanoparticles on the catalyst surface determines the hydrogenation activity; the lowest temperature for 100%  $\text{CO}_2$  conversion to  $\text{CH}_4$  was achieved over the catalyst possessing Ru nanoparticles of 2.5 nm diameter (Table 1). Since smaller nanoparticles were not tested in this study, new experiments are required in order to check if the methanation activity can be further increased with a

Table 1 Catalysts, their activity and selectivity for  $\text{CO}_2$  hydrogenation to  $\text{CH}_4$

| Catalysts                                    | $d/\text{nm}$ | $\tau/\text{ml g}^{-1} \text{ s}^{-1}$ | $T/\text{K}$ | $X(\text{CO}_2)/\%$ | $S(\text{CH}_4)/\%$ | Ref. |
|--|---------------|--|--------------|---------------------|---------------------|------|
| Ru/ $\text{TiO}_2$ (B)                       | 2.5           | 0.24                                   | 453          | 100                 | 100                 | 35   |
| Ru/ $\text{TiO}_2$ (W)                       | 9.5           | 0.24                                   | 693          | 100                 | 100                 | 35   |
| Ru/ $\text{TiO}_2$ (G)                       | 5.2           | 0.24                                   | 513          | 100                 | 100                 | 35   |
| Ru/ $\text{TiO}_2$ (B)                       | 3.4           | 0.24                                   | 473          | 100                 | 100                 | 35   |
| Ru/ $\text{TiO}_2$ (B)                       | 5.0           | 0.24                                   | 693          | 100                 | 100                 | 35   |
| Ru/ $\text{TiO}_2$ (B)                       | 6.4           | 0.24                                   | 513          | 100                 | 100                 | 35   |
| $\text{Ce}_{0.97}\text{Ru}_{0.03}\text{O}_2$ | 12.5          |  | 753          | 51                  | 99                  | 36   |
| $\text{Ce}_{0.96}\text{Ru}_{0.04}\text{O}_2$ | 12.5          |  | 723          | 55                  | 99                  | 36   |
| Pd–Mg/ $\text{SiO}_2$                        | 2.0           |  | 723          | 59                  | 95                  | 37   |
| Pd–Ni/ $\text{SiO}_2$                        | 2.0           |  | 723          | 50.5                | 89                  | 37   |
| 10Ni–CZ                                      |               | 43 000 <sup>a</sup>                    | 623          | 85                  | 99.5                | 38   |
| Ni–MCM-41                                    |               | 1.6                                    | 673          | 56                  | 96                  | 39   |

<sup>a</sup> This value is gas space hourly velocity ( $\text{h}^{-1}$ ). B, W, and G mean different methods of catalyst preparation, *i.e.* barrel-sputtering,<sup>40</sup> Conventional impregnation, and impregnation with partial reduction of  $\text{RuO}_x$  to Ru,<sup>41</sup> respectively.

decreased size or whether the size-activity dependence will follow a typical volcano dependence.

Carbon dioxide can also be directly hydrogenated to hydrocarbons analogously to a classical CO-FT synthesis over Co- and Fe-based catalysts.<sup>34,42,43</sup> However, cobalt catalysts do not follow a typical Anderson-Schulz-Flory distribution in a CO<sub>2</sub>-H<sub>2</sub> feed; methane is the main product.<sup>44,45</sup> This is probably related to the low activity of Co-based catalysts for the generation of CO *via* the RWGS reaction. As summarised elsewhere,<sup>43</sup> CO is an important reaction intermediate in the conversion of CO<sub>2</sub> to higher hydrocarbons over Fe-based catalysts. Such materials have been intensively applied for the CO<sub>2</sub>-FT reaction. The most relevant results up to 2011 have been thoroughly reviewed.<sup>34,43</sup> It should be stressed that unpromoted Fe-based catalysts are not selective for the desired FT products.<sup>34</sup> Mn, Cu, K, and Ce are the most intensively investigated dopants which positively influence the selectivity to higher hydrocarbons. From a mechanistic point of view, both Mn<sup>46,47</sup> and Cu<sup>46</sup> improve the reducibility of FeO<sub>x</sub> species, the distribution of iron species, and the surface basicity. The positive effect of Mn is only valid in a limited concentration range due to blockage of active iron sites at high Mn loadings.<sup>47,48</sup> In contrast, high amounts of K are beneficial for CO<sub>2</sub>-FT in terms of decreasing CH<sub>4</sub> formation and of improving CO<sub>2</sub> conversion.<sup>43</sup> A possible reason for this effect may be that K enhances the chemisorption of CO<sub>2</sub> and simultaneously decreases the adsorption of H<sub>2</sub>.

The positive role of Ce is related to its good low-temperature RWGS activity. The size of CeO<sub>2</sub> domains and the order of catalyst impregnation with ceria influence the activity and selectivity towards C<sub>2</sub>-C<sub>5</sub> olefins.<sup>49</sup> For example, the catalysts prepared *via* deposition of Fe, Mn, and K on alumina impregnated with ceria showed higher activity and selectivity in comparison to their ceria-free counterparts. In order to benefit from the effects of ceria, it is essential to avoid or minimise blockage of the active catalyst components by ceria. This can be achieved by calcination of the unloaded Ce-containing support at a high temperature.

In summary, although Fe-based catalysts show promising results for CO<sub>2</sub>-FT, their performance, in terms of their activity and of the formation of undesired methane, should be further improved. Another possibility to improve the economic feasibility of converting CO<sub>2</sub> to higher hydrocarbons is to initially convert CO<sub>2</sub> to CO and then performing CO-FT. Graves *et al.*<sup>50</sup> analysed the energy balance and economy of fuel production for CO<sub>2</sub> *via* three main steps: (i) CO<sub>2</sub> capture, (ii) conversion of H<sub>2</sub>O and CO<sub>2</sub> to syngas, and (iii) classical FT synthesis. Their process scheme is shown in Fig. 4.

The activation of CO<sub>2</sub> and H<sub>2</sub>O is the most energy demanding part and dominates the process costs. In order to decrease the costs, these authors suggested using the heat of the FT synthesis to preheat the CO<sub>2</sub> and H<sub>2</sub>O for reducing the thermo neutral voltage and thus increasing the overall system efficiency. According to their estimations, the so-produced synthetic fuel could be competitive with gasoline at around 0.53 \$ L<sup>-1</sup> if the electricity price was less than 0.03 \$ kW h<sup>-1</sup> from a constant power supply. For comparison, recent average electricity prices in the USA are approximately 3 times higher. The

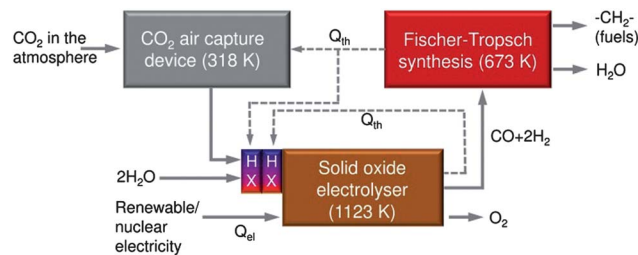


Fig. 4 Process diagram for CO<sub>2</sub> conversion to liquid fuels. Adapted from ref. 50.

cost of CO<sub>2</sub> capture also contributes to the price of fuel, which increases by 0.02 \$ L<sup>-1</sup> with a cost of 0.1 \$ per ton of CO<sub>2</sub> captured. Therefore, it is highly important to reduce electricity costs significantly in order to improve the economics of such CO<sub>2</sub>-based fuel production technology and to make it competitive for the current fossil fuel based technologies.

### Formation of oxygenates from CO<sub>2</sub>

Methanol is an important intermediate for the large-scale production of a variety of chemicals.<sup>51</sup> It is currently produced *via* the hydrogenation of CO over catalysts based on metals and oxides of copper and zinc. These materials can also catalyse the conversion of CO<sub>2</sub> to methanol. Approximately 30 years ago, Lurgi GmbH had already developed and tested a process for the hydrogenation of carbon dioxide to methanol.<sup>52</sup>

In late 2011, the company Carbon Recycling International (CRI) in Iceland commissioned the first plant for methanol production from CO<sub>2</sub>.<sup>53</sup> The production capacity of the plant is around 4 kt of methanol per year, although no information about the type of catalyst or reactor has been disclosed. This year, CRI has already shipped methanol to the Dutch oil company Argos in Rotterdam. CRI also plans to build a new plant with an annual production of methanol of around 40 kt. All CO<sub>2</sub> used in the production process is captured from flue gases from the nearby HS Orka geothermal power plant. This power plant also produces hydrogen through electrolytic water splitting (eqn (4)). From an environmental point of view, the whole production process is clean, with oxygen being the only by-product.

A recent joint contribution from Air Liquide Forschung und Entwicklung GmbH and Lurgi GmbH<sup>54</sup> deals with the technical aspects of the hydrogenation of CO<sub>2</sub> to methanol over a commercial methanol synthesis catalyst from Süd-Chemie. For comparative purposes, methanol production from CO was also investigated on the same catalyst. Catalytic tests were performed in a loop reactor under conditions close to those of large-scale methanol production;  $T_{\text{reactor}} = 523$  K, the gas hourly space velocity was 10 500 h<sup>-1</sup>, total pressure was 80 and 70 bar for CO<sub>2</sub> and CO hydrogenation, respectively. The feed components were separated from the reaction products at the reactor outlet and then recycled. The *per-pass* conversion of CO<sub>2</sub> ranges from 35 to 45%. The catalyst slightly deactivated within the first 100 h on-stream and showed stable operation over the following 600 h. The space-time-yield (STY) of methanol was around 0.6 kg<sub>CH<sub>3</sub>OH</sub> L<sub>cat</sub><sup>-1</sup> h<sup>-1</sup>. This value is approximately 45% lower

than for the CO-based process. This is probably related to the negative effect of H<sub>2</sub>O on the rate of methanol formation when using a CO<sub>2</sub>-H<sub>2</sub> feed. Actually, several previous studies have claimed that the kinetics of CO<sub>2</sub> hydrogenation are faster than the kinetics of CO hydrogenation.<sup>55–58</sup> CO was suggested to remove oxygen species coming from H<sub>2</sub>O. Another important difference between the CO- and CO<sub>2</sub>-based production of methanol relates to the product selectivity. Compared to the former process, the latter shows significantly higher water content but notably lower selectivity towards carbon-containing products, like higher alcohols, hydrocarbons, esters, and ketones.

Dimethyl ether (DME) is another important chemical, with potential as a substitute for conventional diesel. It can be formed from CO<sub>2</sub> in a single-step process using a bifunctional catalyst, *i.e.* when a methanol synthesis catalyst is combined with an acid catalyst like  $\gamma$ -Al<sub>2</sub>O<sub>3</sub> or zeolites. Alternatively, methanol is formed in one reactor followed by its further dehydration to DME in another reactor. Since DME formation is thermodynamically limited due to the negative effect of water formed upon methanol dehydration, pure (distilled) methanol is typically used. The distillation step is an important cost factor. Recently, Lurgi developed the MegaDME® process,<sup>54</sup> which can tolerate methanol streams with a high water content. Fig. 5 gives an overview of the main process operations. This process features energy integration through the coupling of the methanol vaporizer and the DME-column, an arrangement which saves the investment costs for these two individual operation units because the methanol vaporizer and the DME-column can become the reboiler or overhead condenser of each other.<sup>54</sup>

**Catalysts.** Apart from the availability of large amounts of cheap and pure CO<sub>2</sub> and H<sub>2</sub>, the relatively low productivity of methanol is also an important issue. Therefore, many research

groups try to elucidate factors determining catalyst activity, selectivity, and time-on-stream stability. In general, the most active and selective catalysts contain Cu as the main active component together with different modifiers.<sup>34,59,60</sup> ZnO is an important supporting material used for preparation of Cu-containing catalysts. The value of ZnO is its ability to control the morphology and stabilise the copper species.<sup>61,62</sup> It is well established that the activity and selectivity can be improved when ZnO is promoted by ZrO<sub>2</sub>,<sup>63–65</sup> Al<sub>2</sub>O<sub>3</sub>,<sup>66–68</sup> La<sub>2</sub>O<sub>3</sub>,<sup>59</sup> or SiO<sub>2</sub>.<sup>69</sup> The promoting effect is often related to a better dispersion of copper species. In addition, structural characteristics of supports play an important role. For example, Guo *et al.*<sup>64</sup> applied a glycine-nitrate combustion method to prepare Cu-ZnO-ZrO<sub>2</sub> catalysts and tested them for the conversion of CO<sub>2</sub> to methanol at 493 K and 30 bar. These authors found a linear correlation between turnover-frequency (TOF) and the relative amount of monoclinic zirconia in the catalysts. Based on these results and previous studies by Bell and coworkers,<sup>70</sup> Cu species on monoclinic zirconia were suggested to possess a higher concentration of carbon-containing intermediates yielding methanol. However, this is probably not the only activity-determining factor. Later, the same authors were unable to establish a direct relationship between the TOF values of methanol formation and the content of monoclinic zirconia in Cu-ZnO-ZrO<sub>2</sub> catalysts prepared *via* the solid-state reaction route.<sup>65</sup> The monoclinic zirconia was suggested to be relevant for methanol selectivity. In order to avoid such contradictive discussions, additional systematic studies are required to further elucidate the role of zirconia morphology in the hydrogenation of CO<sub>2</sub> to methanol.

The effect of support morphology was also established in the conversion of CO<sub>2</sub> to methanol over a physical mixture of Cu with rod-like or plate-like ZnO and Al<sub>2</sub>O<sub>3</sub>.<sup>71</sup> When the plate-like

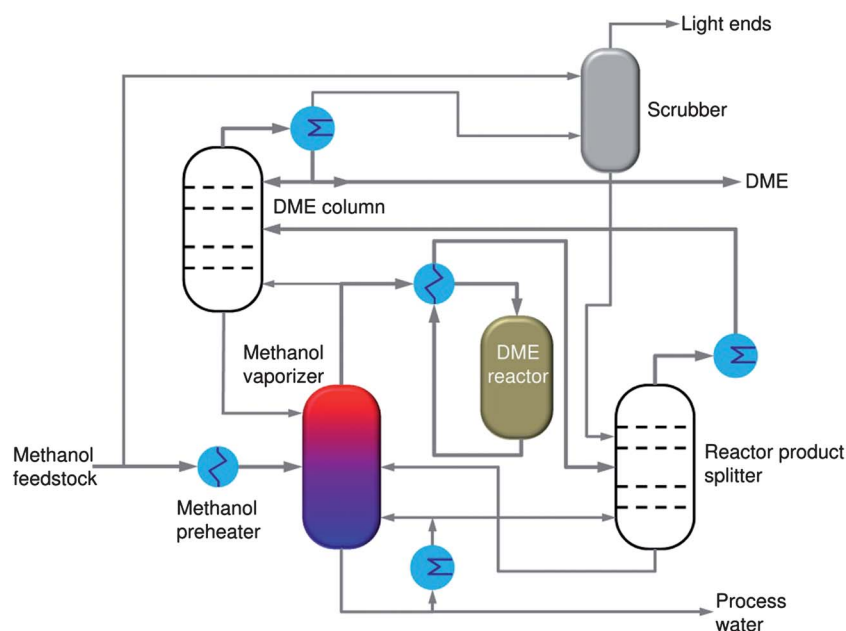


Fig. 5 MegaDME® basic process instrumentation diagram taken from ref. 54.

ZnO crystals were used, significantly higher methanol selectivity at a slightly lower CO<sub>2</sub> conversion was achieved compared to the catalysts based on the rod-like ZnO. The authors of ref. 71 concluded that additional oxygen vacancies are formed at the Cu–ZnO interface when copper interacts with ZnO crystals of plate-like morphology. These vacancies were suggested to be active sites for CO<sub>2</sub> activation.

Pd<sup>72–76</sup> and Au-containing<sup>77</sup> materials were also tested for the hydrogenation of CO<sub>2</sub> to methanol. Liang *et al.*<sup>72</sup> showed that active catalysts for the above reaction were obtained by supporting Pd/ZnO on carbon nanotubes. The nanotubes play a dual role: they (i) help to increase the dispersion of metallic Pd and (ii) are additionally able to adsorb hydrogen. A similar effect of carbon nanotube supports on the catalytic properties of a Pd/Ga<sub>2</sub>O<sub>3</sub> system was also established.<sup>73</sup> Very recently, Zhou *et al.*<sup>76</sup> have demonstrated that both the CO<sub>2</sub> conversion and methanol selectivity exhibited by supported Pd species are strongly influenced by the exposed face of the β-Ga<sub>2</sub>O<sub>3</sub> support. The best performance was obtained over Pd supported on the (002) facet. This is due to the fact that this surface helps to increase the dispersion of Pd owing to the strong metal–support interaction. Another example of the importance of support morphology for methanol synthesis is the hydrogenation of CO<sub>2</sub> on Au/TiC(001) and Cu/TiC(001).<sup>77</sup> The metal-normalized activity of these materials was significantly higher than that of Cu(111) under ultrahigh vacuum conditions. This was explained by a charge polarization of Au and Cu particles, which activates them for the reaction.

**Mechanistic aspects of CO and CO<sub>2</sub> hydrogenation to methanol.** From a mechanistic point of view, the catalytic hydrogenation of CO<sub>2</sub> to methanol can occur directly or indirectly with participation of CO formed through the RWGS reaction. In the former, two alternative mechanistic schemes are suggested. They differ in the key reaction intermediates, which are formate (HCOO) or hydrocarboxyl (COOH) species. To identify possible elementary reaction pathways of direct hydrogenation of CO<sub>2</sub> to methanol, periodic DFT calculations were performed on Cu(111),<sup>78,79</sup> Cu(211)<sup>66</sup> and CuZn(211).<sup>66</sup> The hydrogenation of CO to methanol was also calculated to clarify if the mechanistic concepts of CO- and CO<sub>2</sub>-based methanol synthesis differ. Considered reaction networks of methanol formation are shown in Fig. 6.

The hydrogenation of CO<sub>2</sub> starts with the non-dissociative and dissociative adsorption of CO<sub>2</sub> and H<sub>2</sub>. Subsequently, the adsorbed CO<sub>2</sub> species are hydrogenated step-wise to adsorbed HCO, H<sub>2</sub>CO, H<sub>3</sub>CO, and finally to H<sub>3</sub>COH. Owing to the very weak adsorption of CO<sub>2</sub>, it was suggested to react directly from the gas phase with adsorbed H species to yield *mono*-HCOO or *trans*-COOH adsorbed species.<sup>78</sup> The latter species were not considered by Behrens *et al.*<sup>66</sup> and Grabow *et al.*<sup>79</sup> Irrespective of the exposed face of the Cu surface and of the co-existence of Zn, formate species can be preferably hydrogenated to HCOOH. A common adsorbed CH<sub>2</sub>O intermediate was found to be involved in the hydrogenation both of CO and CO<sub>2</sub> to methanol. In general, the stability of the CO<sub>2</sub> hydrogenation intermediate species is energetically favoured, albeit with a larger activation

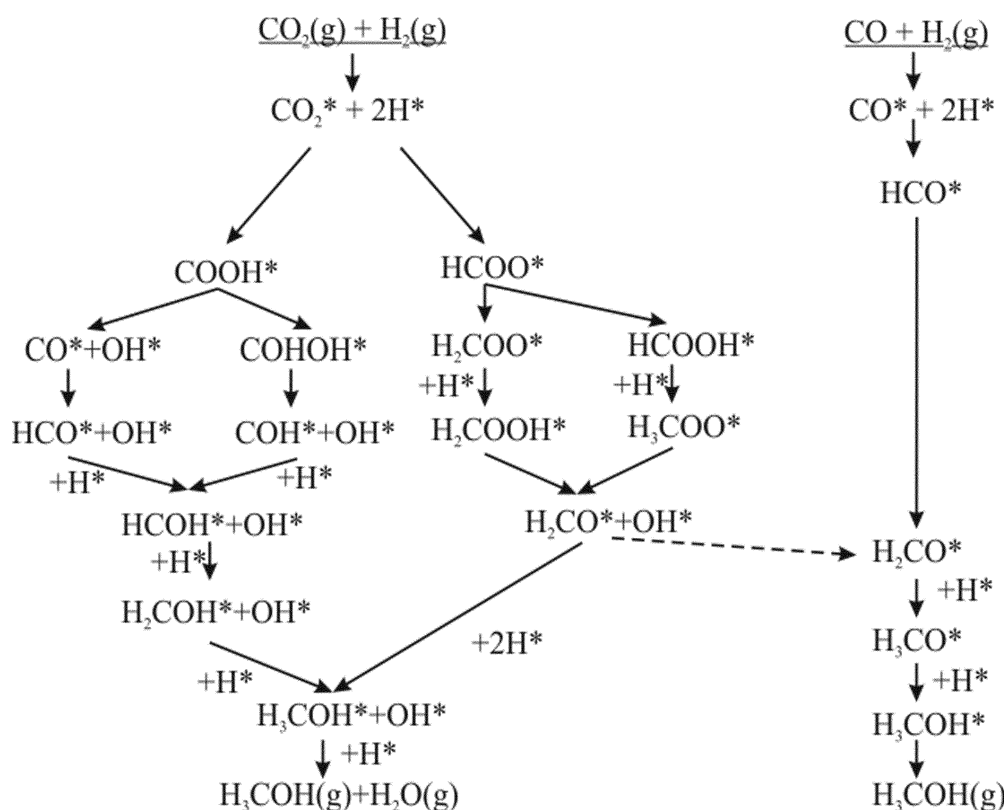


Fig. 6 Pathways for methanol formation from CO<sub>2</sub> and H<sub>2</sub> or CO and H<sub>2</sub> on metallic Cu. \* represents a surface Cu site. Adapted from ref. 66, 78 and 79.



barrier than in the case of CO. Another important conclusion is that CO is not only used as a promoter for CO<sub>2</sub> hydrogenation to methanol, but is also hydrogenated in significant amounts *via* the common CH<sub>2</sub>O intermediate.

In contrast to the above studies, Zhao *et al.*<sup>78</sup> excluded methanol formation from CO<sub>2</sub> *via* the formate route because the surface HCOOH species either easily desorb or dissociate back into HCOO and H. In addition to formate intermediates,<sup>66,79</sup> these authors also considered hydrocarboxyl (COOH) species. Although the formation of such species is less energetically favourable compared with formate species, Zhao *et al.*<sup>78</sup> predicted that co-adsorbed water helps to stabilise them. They can be further hydrogenated to COHOH species, which decomposes to COH and OH. The former species is transformed to methanol through the addition of three hydrogen atoms. Thus, in order to discriminate between reaction pathways leading to methanol directly from CO<sub>2</sub>, experimental studies on surface intermediates or independent DFT calculations are highly desired. They must include the effects of the secondary reactions, such as RWGS, and their adsorbed intermediates, especially those involved in H<sub>2</sub>O formation.

The key intermediates may also depend on the structure of the catalytically active Cu surface. A recent combined experimental and theoretical study established that the sites active in methanol synthesis comprise Cu steps decorated with Zn atoms.<sup>66</sup> The authors used industrial Cu/ZnO-based catalysts for methanol synthesis at 60 bar and 483 and 523 K. The main conclusion of their thorough catalyst characterization was related to the role of bulk defects in inducing line defects at the

exposed surfaces of Cu. In their DFT calculations, stepped Cu(211) and flat Cu(111) surfaces were used to elucidate the role of surface defects in the hydrogenation of both CO and CO<sub>2</sub> to methanol. For the hydrogenation of CO<sub>2</sub> only the formate route was considered. In agreement with ref. 78, formate species are weakly bound on the flat Cu(111) surface. Adsorption energies of surface intermediates in CO- and CO<sub>2</sub>-based methanol synthesis are strengthened upon elevating the pressure of feed components. Independently, both the intermediate and the transition state energies were stabilised on the stepped Cu(211) surface, explaining its higher intrinsic activity compared to that of the flat Cu(111) surface. In addition, allowing for the introduction of Zn into the Cu step further increased the adsorption strength of HCO, H<sub>2</sub>CO, and H<sub>3</sub>CO intermediates and decreased the activation barriers. From these DFT data, an active catalyst for the synthesis of methanol from CO<sub>2</sub> should possess Cu nanoparticles with a high step density and Zn atom nearby.

## Electrocatalytic CO<sub>2</sub> hydrogenation

### Electrodes and reaction cells

The electrocatalytic reduction of CO<sub>2</sub> has a long history dating from the 19<sup>th</sup> century. Since the last three decades, this topic has attracted interest from both academia and industry. CO<sub>2</sub> can be electrocatalytically converted into various products directly at the surface of solid electrodes. Alternatively, a homogeneous catalyst, which also participates in an electron transfer reaction from solid electrodes, can be additionally

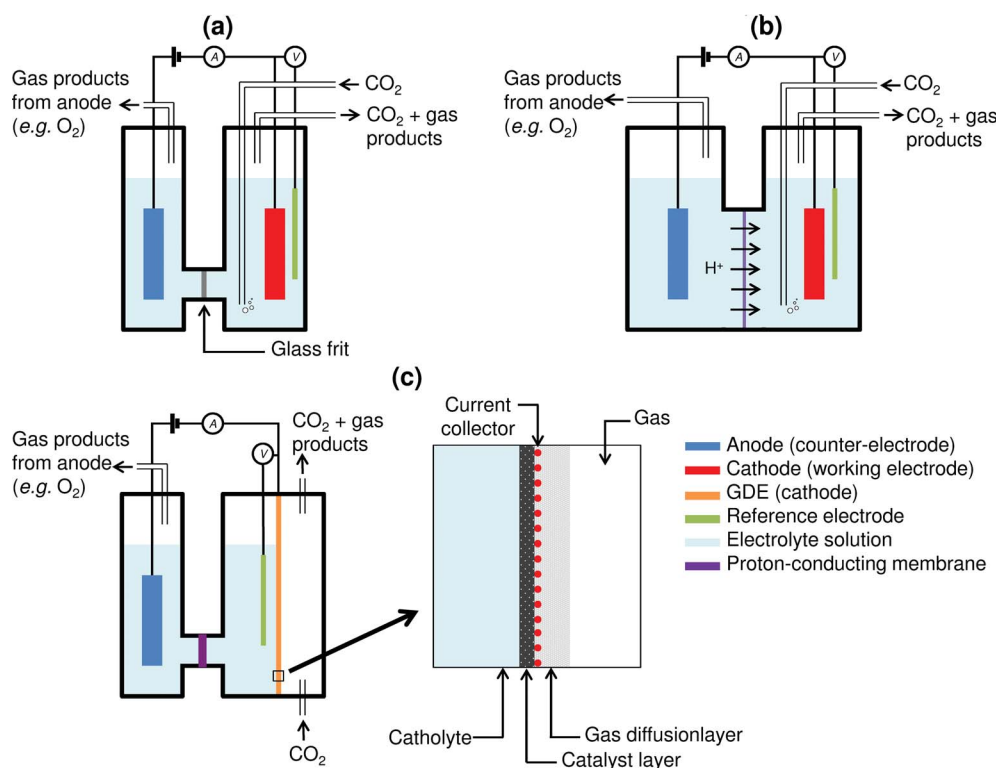


**Fig. 7** Laboratory cells used for electrochemical CO<sub>2</sub> conversion: (a) two-compartment cell, (b) cell with electrodes separated by an H<sup>+</sup>-conducting membrane, and (c) cell with a gas diffusion electrode.

incorporated to convert the CO<sub>2</sub>. A number of reviews have been published covering various aspects of CO<sub>2</sub> reduction.<sup>11–14,80–84</sup> Herein, we cover recent advances in this fast developing research area of direct CO<sub>2</sub> conversion over metal electrodes. A brief general description of electrocatalytic cells, reaction conditions, and electrodes will be concisely described. Fig. 7 shows schemes of cells often used for CO<sub>2</sub> conversions. As highlighted by Hori,<sup>83</sup> the cells must also enable appropriate chemical analysis of the products formed at the electrodes. A significant number of experiments were performed in standard cells with undivided electrodes (Fig. 7).

Common methods used for testing CO<sub>2</sub> reduction are summarised elsewhere.<sup>14</sup> This paper also contains information about the effect of temperature, pressure and pH on the rates of CO<sub>2</sub> reduction and product distribution. In general, an increase in the pressure and a decrease in the temperature result in higher reaction rates owing to an increased CO<sub>2</sub> concentration in the electrolyte. The application of nonaqueous solutions also improves CO<sub>2</sub> solubility and suppresses the hydrogen evolution reaction.<sup>83</sup> Various metals as well as carbon and boron were applied as cathodes. Lvov *et al.*<sup>14</sup> summarised studies dealing with the individual electrodes. According to Hori and coworkers,<sup>83,85,86</sup> simple metal electrodes can be classified in four groups depending on the type of reaction products (Fig. 8). Metallic Cu is the only member of the first group and shows exceptional selectivity and activity for CO<sub>2</sub> conversion to hydrocarbons. The second group consists of Au, Ag and Zn, which yield CO as the main product. The third group, including In, Pb, Sn and Cd, is characterized by the formation of formate as the main product, while hydrogen evolution was almost exclusively observed over Ni, Fe, Pt and Ti electrodes. It is interesting to note that CO is adsorbed very strongly on metals of the fourth group; it has been postulated that the adsorbed CO prevents further reduction of CO<sub>2</sub>, hence resulting in hydrogen evolution.<sup>86</sup> Another study,<sup>87</sup> performed at  $-2.2$  V vs. SCE (standard calomel electrode) in a 0.05 M KHCO<sub>3</sub> solution at 273 K, found the following electrodes to be mostly inactive in CO<sub>2</sub> reduction: C, Al, Si, V, Cr, Mn, Fe, Co, Zr, Nb, Mo, Ru, Rh, Hf, Ta, W, Re and Ir.

In the works cited above, structurally simple electrodes were used. For instance, a typical Cu electrode was prepared by

cutting a strip out of an ultrapure copper sheet, which was then mechanically polished with fine emery paper and electropolished in 85% phosphoric acid.<sup>85</sup> Electropolishing is commonly used to brighten the surface and remove irregularities after the mechanical polishing. However, later studies have highlighted the influence of the surface morphology of the electrode and the preparation method. Cook *et al.*<sup>88</sup> reported a current efficiency of 73% for CH<sub>4</sub> and 25% for C<sub>2</sub>H<sub>4</sub> at 8.3 mA cm<sup>-2</sup> on an electrode prepared by the *in situ* electrodeposition of copper on a glassy carbon substrate in 0.5 M KHCO<sub>3</sub> at 273 K. Even at 25 mA cm<sup>-2</sup> the overall Faradaic efficiency for these two products was 79%. Likewise, studies with single crystal electrodes have demonstrated that different surface faces display different activity and selectivity in electrocatalytic CO<sub>2</sub> reduction. Single crystal Cu electrodes dominated by Cu(100) faces favour C<sub>2</sub>H<sub>4</sub> formation, while those dominated by Cu(111) faces show enhanced selectivity towards CH<sub>4</sub>.<sup>89</sup> Cu(110) faces demonstrate increased yields of alcohols and non-gaseous C<sub>2</sub> and C<sub>3</sub> products in comparison with others.

Despite the many advances in aqueous CO<sub>2</sub> reduction, the process remains challenging due to (i) the high overpotential (the difference between the thermodynamic and actual electrode voltages to drive a reaction) required, (ii) the low solubility of CO<sub>2</sub> in water at ambient temperature and pressure, (iii) the formation of a mixture of products implying a costly separation step, and (iv) the fouling and deactivation of the electrodes by impurities. These issues can be partly addressed by employing gas diffusion electrodes (GDEs). A GDE usually consists of a Teflon-bonded carbon black matrix on which metal catalyst particles are dispersed. Their application for CO<sub>2</sub> reduction was first demonstrated by Mahmood *et al.*,<sup>90</sup> who employed a lead-impregnated GDE to reduce CO<sub>2</sub> to formic acid with a current efficiency of nearly 100% at a current density of 150 mA cm<sup>-2</sup> and a potential of approximately  $-1.8$  V vs. SCE. Hara *et al.*<sup>91</sup> reported that a platinum GDE produced methane from CO<sub>2</sub> at 30 bar with a Faradaic efficiency of 34.8% at a current density of 900 mA cm<sup>-2</sup>.

While traditional electrochemical cells are appropriate for fundamental research on the electrocatalytic reduction of CO<sub>2</sub>, it is clear that practical applications would require more complex systems. Similarly, for practical purposes it is important to regard the reduction of CO<sub>2</sub> not just as an individual reaction, but as part of the overall cell in which valuable products are also obtained from the oxidation reaction. Kobayashi and Takahashi<sup>92</sup> demonstrated a low-density energy cell, which produced methanol from CO<sub>2</sub> and H<sub>2</sub> at ambient pressure with up to 97% current efficiency at a potential of  $-0.1$  V vs. the standard hydrogen electrode. The anodic and cathodic half cells were separated using a cation exchange membrane (Nafion 117). H<sub>2</sub> was supplied to the anodic part consisting of a Pt/C catalyst, while the cathode, which was bubbled with CO<sub>2</sub> in a 0.1 M KHCO<sub>3</sub> electrolyte, consisted of a Cu/Zn/Al catalyst applied to the other side of the membrane. Electron transfer between the electrodes occurred *via* an external circuit while the membrane allowed the transport of protons from the anode to the cathode. Yamamoto *et al.*<sup>93</sup> first reported the production of synthesis gas from CO<sub>2</sub> reduction and oxygen from water oxidation in a cell employing Ni/active carbon fibre and Cu/metal oxide GDEs. Several cells for

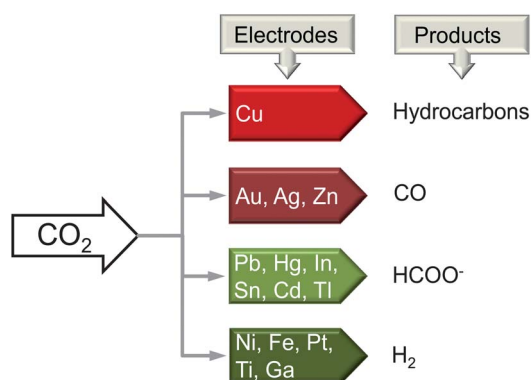


Fig. 8 Electrode materials and reaction products of CO<sub>2</sub> reduction. Adapted from ref. 83.

the electrochemical production of synthesis gas from CO<sub>2</sub> have been reported in the past few years. Newman *et al.*<sup>94</sup> developed and tested several cell designs based on proton exchange membrane fuel cells (PEMFCs) for the simultaneous reduction of CO<sub>2</sub> and H<sub>2</sub>O to syngas. The best results were obtained in a “modified” PEMFC by inserting a glass fibre-supported layer of aqueous KHCO<sub>3</sub> between the proton-exchange membrane (Nafion) and the silver-based catalyst cathode layer. This cell produced syngas with a CO : H<sub>2</sub> ratio of 1 : 2 at a potential of −2 vs. SCE and a total current density of 80 mA cm<sup>−2</sup> at 298 K, while O<sub>2</sub> was obtained at the anode. Dufek *et al.*<sup>95</sup> demonstrated a bench-scale flow cell-based device fitted with an Ag GDE as the cathode and a commercial Ru-based anode separated by a Nafion 424 cation-exchange membrane. Interestingly, the cell was operated at 344 K, which the authors felt would more closely resemble the conditions of an actual commercial cell, and they found that the CO : H<sub>2</sub> ratio of the syngas produced could be controlled between 4 : 1 and 1 : 9 by adjusting the flow of CO<sub>2</sub> and the current density. The same group recently reported a similar system to continuously produce CO from CO<sub>2</sub>.<sup>96</sup> Operating at 18.5 bar, this system was able to produce CO with a current efficiency of up to 92% at 350 mA cm<sup>−2</sup>. The cell voltage decreased with increasing temperature, dropping below 3 V at 363 K. At this temperature an electrical efficiency of 50% at 225 mA cm<sup>−2</sup> was observed. Narayanan *et al.*<sup>97</sup> reported a cell for converting CO<sub>2</sub> to formate with high current efficiency (*ca.* 80%) using sodium ion- or hydrogen-ion-conducting membranes.

### Improving performance of metal electrodes

None of the investigated electrodes perform better than Cu for CO<sub>2</sub> reduction in aqueous solutions in terms of activity and time-on-stream stability. However, even the latter electrodes suffer from high overpotentials and low current densities. In addition, when CO<sub>2</sub> reduction is coupled with H<sub>2</sub>O oxidation, the overpotential for CO<sub>2</sub> conversion to hydrocarbons increases. Water electrolysis is a benchmark for electrocatalytic CO<sub>2</sub> reduction. As demonstrated by Whipple and Kenis,<sup>14</sup> until 2010 the efficiency (eqn (5)) of electrodes used for the latter approach was still very low compared to the water electrolysis (Fig. 9).

$$E_{\text{energetic}} = \frac{E^0}{E^0 + \eta} \times E_{\text{Faradaic}} \quad (5)$$

where  $E^0$ ,  $\eta$  and  $E_{\text{Faradaic}}$  are standard potential, overpotential, and Faradaic efficiency, respectively.

To circumvent these problems, several strategies were suggested and are briefly discussed below. They include: (i) modifying metal electrodes with corresponding oxides, (ii) operating at high temperature with molten or solid-oxide electrolytes, (iii) applying photo irradiation, (iv) using ionic liquid electrolytes (water-free conditions), or (v) biological microorganisms. The three latter aspects are discussed in the “Alternative approaches to electrocatalytic CO<sub>2</sub> conversions” section.

### Modification of metal electrodes

Goncalves *et al.*<sup>100</sup> demonstrated the importance of electro-depositional modification of copper electrodes for the

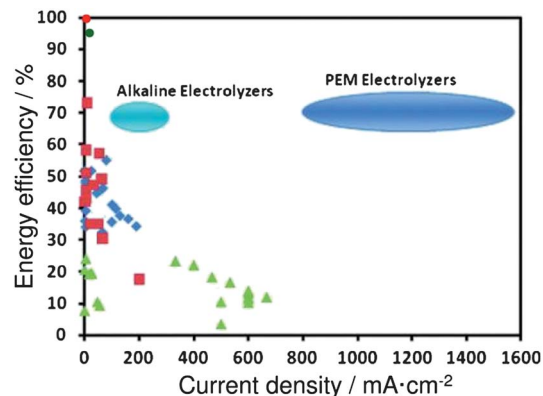


Fig. 9 Comparison of the energy efficiencies and current densities for CO<sub>2</sub> reduction to formic acid (◆), syngas (■), and hydrocarbons (▲). This figure is from ref. 13. ● and ● represent the data for CO<sub>2</sub> reduction to methanol<sup>98</sup> and CO<sup>99</sup> respectively.

reduction of CO<sub>2</sub> to hydrocarbons. A copper mesh cathode produced methane and ethylene with a similar selectivity. Two modified copper electrodes from Omnidea Lda possessed approximately 7 and 19 times higher specific surface area than the unmodified one. They also showed significantly lower selectivity towards methane in favour of ethylene and ethane. Unfortunately, these authors did not explain how they modified their electrodes. Electrodeposition of a thin layer of Cu<sub>2</sub>O on Cu electrodes was reported to change the product selectivity from hydrocarbons to methanol.<sup>101</sup> It was suggested that Cu<sup>+</sup> plays an important role in the production of methanol. However, Li and Kanan<sup>102</sup> recently showed that Cu was the active component of copper electrodes initially precovered with a thick layer of Cu<sub>2</sub>O. These authors investigated the effect of the layer thickness on the CO<sub>2</sub> reduction activity to CO and HCO<sub>2</sub>H. It is important to stress that copper oxide was reduced to metallic copper after the electrode had been used for CO<sub>2</sub> reduction. High activity and time-on-stream stability were achieved when the layer was thicker than approximately 3 μm. This was explained by the fact that certain Cu particles are formed upon reduction of the thick Cu<sub>2</sub>O layer during electrolysis. Such *in situ* formed electrodes converted CO<sub>2</sub> to CO and HCO<sub>2</sub>H with the Faradaic efficiencies of 45 and 33%, respectively, at potentials between −0.3 and −0.65 V vs. the reversible hydrogen electrode. Polycrystalline Cu electrodes were inert under the same reaction conditions.

The group of Kanan<sup>103</sup> also reported an increased activity using a Sn/SnO<sub>2</sub> electrode for CO<sub>2</sub> reduction compared with a Sn electrode. CO and HCO<sub>2</sub>H were the only reaction products formed over both electrodes. However, the Faradaic efficiency of the Sn/SnO<sub>2</sub> electrode for CO and HCO<sub>2</sub>H formation was 4 and 3 times higher than that of the Sn electrode, respectively. The role of SnO<sub>x</sub> layer was suggested to be related to the stabilisation of CO<sub>2</sub><sup>−</sup>, which was further converted to HCOOH and CO. From a mechanistic point of view, it is still not clear if the conversion takes place on Sn<sup>0</sup> or SnO<sub>x</sub>.

An interesting approach for CO<sub>2</sub> reduction was reported by Chen *et al.*<sup>104</sup> These authors combined water oxidation by simple inorganic Cu<sup>2+</sup> salts with the electrocatalytic reduction of CO<sub>2</sub> on a Cu(0) nanoparticulate film. Their electrochemical

cell consisted of two chambers filled with a 0.1 M NaHCO<sub>3</sub> solution saturated with CO<sub>2</sub> at 1 bar. They were separated by a Nafion membrane. One chamber contained a boron-doped diamond (BDD) disk anode in the presence of 1.2 mM CuSO<sub>4</sub>. The cathode chamber was equipped with a high-surface area metallic Cu electrode deposited on a BDD disk. The reaction products were CO, HCOO<sup>-</sup>, H<sub>2</sub> and O<sub>2</sub>. When the electrolysis was performed in the same cell but in the absence of the Cu<sup>2+</sup> salt, the amount of reaction products was significantly lowered at *ca.* 3 times lower current density.

In summary, CO<sub>2</sub> reduction catalysed by metal electrodes still suffers from low Faradaic efficiencies and current densities. Further improvements in this field are expected as the mechanistic role of metal and metal oxides in the reduction process is better understood. This will open the possibility to design electrodes with certain compositions.

### Solid-oxide electrolytes

Compared with electrochemical cells operating in the liquid phase and at ambient temperature, performing electrolysis at high-temperatures (>673 K) is thermodynamically and kinetically more attractive. Such electrolyzers operate with molten carbonate or solid-oxide electrolytes. The latter cells typically use zirconia stabilised by yttrium oxide as the electrolyte. Relevant references for electrolysis of CO<sub>2</sub> or H<sub>2</sub>O can be found in a recent review.<sup>50</sup> Since 2009, several papers have appeared dealing with the co-electrolysis of H<sub>2</sub>O and CO<sub>2</sub> to produce syngas.<sup>105–111</sup> However, all these studies used a feed containing H<sub>2</sub> in addition to H<sub>2</sub>O and CO<sub>2</sub>. As a consequence, a source of hydrogen is required. Moreover, a part of CO is produced *via* the RWGS reaction and not by co-electrolysis of CO<sub>2</sub> and H<sub>2</sub>O.<sup>107</sup> As reported by Hu *et al.*,<sup>108</sup> H<sub>2</sub> co-feeding is not required to directly produce paraformaldehyde from CO<sub>2</sub> and H<sub>2</sub>O. The activation of the feed components was possible only when the Pt/CaO–ZrO<sub>2</sub> interface was polarised by a DC current or voltage. The maximum CO<sub>2</sub> conversion of up to 8%, with 100% paraformaldehyde selectivity, was obtained at 1173 K with 1.5 V DC voltages.

Proton-conducting electrolyzers which effectively split H<sub>2</sub>O to H<sub>2</sub> and O<sub>2</sub> at high temperatures also have potential for the electrocatalytic reduction of CO<sub>2</sub> as demonstrated by Xie *et al.*<sup>110</sup> These authors used a BaCeO<sub>0.5</sub>Zr<sub>0.3</sub>Y<sub>0.16</sub>Zn<sub>0.04</sub>O<sub>3–δ</sub> electrolyte to convert CO<sub>2</sub> into CO and CH<sub>4</sub> in the presence of H<sub>2</sub> and H<sub>2</sub>O. The reaction feeds containing CO<sub>2</sub> and H<sub>2</sub>/H<sub>2</sub>O were separately supplied to the cathode and anode compartments, respectively. A CO<sub>2</sub> conversion of 65% was obtained at 887 K and at a current density of 1.5 A cm<sup>-2</sup>, which is attractive from an application viewpoint. Unfortunately, the Faradaic efficiency of CH<sub>4</sub> was only 2.4% in contrast to 29.5% for CO formation. This is probably due to the fact that CO<sub>2</sub> reduction to CO is faster than hydrogen transport through the electrolyte leading to an unfavourable CO<sub>2</sub>/CO ratio on the cathode side to yield CH<sub>4</sub>.

### Alternative approaches to electrocatalytic CO<sub>2</sub> conversions

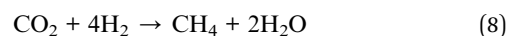
Barton *et al.*<sup>112</sup> demonstrated the highly selective reduction of CO<sub>2</sub> to methanol in water when using a p-GaP semiconductor electrode with pyridine as a co-catalyst. Methanol was observed

only in the presence of pyridine when the electrode was irradiated with a 200 W Hg–Xe arc light source. It is important to highlight that pyridine was not consumed over the experimental time, supporting its catalytic action. In this cell, the electrode utilises light energy for CO<sub>2</sub> reduction to methanol without any other external energy input. The reduction of methanol at pH 5.2 was performed at –0.4 V *vs.* SCE with Faradaic efficiencies reaching 100% at a current density of 0.5 mA cm<sup>-2</sup>. According to ref. 113, the rate of methanol formation is affected by (i) the Lewis acidity of the pyridyl nitrogen and (ii) the ability of the electrode surface to stabilise carbon-based free radicals. Further mechanistic aspects of methanol formation from CO<sub>2</sub> in the presence of pyridine are thoroughly discussed in the “Co-catalysts” section.

The application of an ionic liquid (1-ethyl-3-methylimidazolium) electrolyte was found to be favourable for the electrocatalytic reduction of CO<sub>2</sub> to CO.<sup>99</sup> The tests were performed in a continuous flow cell equipped with a Pt anode and an Ag cathode separated by this ionic liquid. The ionic liquid behaves as a co-catalyst lowering the potential for formation of the CO<sub>2</sub><sup>-</sup> intermediate. H<sub>2</sub> and CO were the only reaction products formed at the cathode, while O<sub>2</sub> was formed at the anode. The amount of hydrogen produced was very low proving the minor occurrence of water electrolysis. The Faradaic efficiency was around 100% at overpotentials below 0.2 V, *i.e.* 87% energy efficiency. This is actually the highest reported value for CO formation. The turnover frequency for CO formation rose from 0.8 s<sup>-1</sup> to 1.4 s<sup>-1</sup> upon increasing the potential of the cell from 1.5 and 2.5 V. Unfortunately, this resulted in a simultaneous decrease in the energy efficiency from 87 to 50%.

Microbial electrolysis cells (MECs) appear to be attractive devices for the reduction of CO<sub>2</sub> to useful products.<sup>114–118</sup> An MEC device consists of an anode and a biocathode separated by a proton-exchange membrane. The oxidation of water takes place at the anode resulting in gaseous O<sub>2</sub>. Alternatively, the anode can also contain bacteria oxidizing biological substrates to CO<sub>2</sub> with simultaneous generation of electrons and protons. In both cases, the protons and electrons generated flow to the cathode through the membrane and an external electrical circuit, respectively. Reaction products are formed at cathodic sites *via* CO<sub>2</sub> hydrogenation with the help of electrochemically active microorganisms.

In their pioneering work, Cheng *et al.*<sup>114</sup> used *Methanobacterium palustre* to selectively produce CH<sub>4</sub> from CO<sub>2</sub> in a MEC with an electron capture efficiency of 96%. Mechanistically,<sup>115</sup> CH<sub>4</sub> is formed *via* two reaction pathways: (i) direct extracellular electron transfer processes (eqn (6)) or (ii) biological CO<sub>2</sub> reduction with H<sub>2</sub> formed from water (eqn (7) and (8)). The relative contribution of these processes depends on the cathode potential. The extracellular electron transfer route showed the highest contribution to the overall methane production at –0.75 V.



To estimate the potential of the MEC approach for CO<sub>2</sub> hydrogenation to CH<sub>4</sub>, Van Eerten-Jansen *et al.*<sup>117</sup> performed a long-term test for *ca.* 200 days. Two different anolytes were tested, *i.e.* hexacyanoferrate(II) and water. The latter showed approximately 8 times lower activity for electron donation. Using water the cell produced methane stably during the operation time at an average rate of  $6 \pm 8 \text{ L (CH}_4\text{) L}^{-1} \text{ day}^{-1}$ . The overall energy efficiency was 3.1%. In order to be competitive with anaerobic digestion processes generating methane, the MEC approach should have the efficiency not worse than 5.5%. Based on previous literature and their own results, these authors<sup>117</sup> defined four possibilities for increasing the energy efficiency: (i) developing active high-surface area electrode materials, (ii) using porous electrodes to increase mass and charge transport, (iii) decreasing the distance between the electrodes and the membrane, and (iv) using membranes with low permeability for gas-phase products. Very recently, an integrated concept for low-voltage CO<sub>2</sub> functionalisation has been suggested.<sup>118</sup> It uses Fe-oxidizing bacteria (*Mariprofundus ferrooxydans*) at the cathode site, which fulfills a double function, *i.e.* catalysing the reduction of CO<sub>2</sub> and acting as a voltage multiplier. Polysaccharides were identified as reaction products of CO<sub>2</sub> fixation by the bacteria. Electrochemically generated Fe<sup>2+</sup> was the sole electron source.

An electromicrobial approach was also suggested for converting CO<sub>2</sub> to higher alcohols.<sup>119</sup> The idea behind this concept was to combine the electrocatalytic reduction of CO<sub>2</sub> to formate in a cell consisting of an In foil cathode and a Pt anode, with the consecutive fermentative conversion of formate to isobutanol and 3-methyl-1-butanol. The latter transformation was catalysed by *Ralstonia* strain LH74D. To avoid degradation of the microbes, the anode was shielded by a porous ceramic cup. This shield quenched reactive intermediates like O<sub>2</sub><sup>-</sup> and NO but did not influence the diffusion of chemicals.

## Photocatalytic CO<sub>2</sub> conversion

### Laboratory photoreactors

Since the advent of photocatalysis in the 1970s a tremendous amount of studies have been reported in the literature focused on photocatalyst synthesis and evaluation in various applications, including environmental remediation, water splitting, CO<sub>2</sub> reduction and synthetic chemistry. Still, very few examples exist of chemical processes operating on the basis of photocatalysis technology. Not only the photon efficiency of materials and the resulting achievable rates remain insufficient to warrant commercial application, also sub-optimal photocatalytic reactors often induce inefficiency and limit the practical application.<sup>120,121</sup> In the construction of a photocatalytic reactor, in addition to mass transfer considerations, the reactor should also be designed to allow optimised exposure of catalytically active sites to light.<sup>122</sup> In particular in slurry reactors scattering properties largely depend on (time dependent) agglomeration phenomena, which will affect rates.<sup>122</sup> Changes in scattering behaviour obviously are less dominant in reactor configurations equipped with coated catalyst systems.<sup>123,124</sup> Still, scattering properties might vary for different coating strategies

leading to different agglomerate sizes and porosities, also making comparison of photocatalytic rates achieved for coated systems difficult. Very little information can be found in the literature on comparing the optical properties of coatings of similar chemical composition, but with different physical appearance.

Solar-to-fuel synthesis, *i.e.* the light-induced reaction of CO<sub>2</sub> and H<sub>2</sub>O to form hydrocarbons, is currently considered a promising technology for the storage of solar energy in the form of chemical bonds.<sup>123</sup> At the same time the technology might contribute to reducing the emission of CO<sub>2</sub>. In laboratory studies describing the photocatalytic CO<sub>2</sub> reduction, batch reactors have usually been applied. In liquid-phase operation, slurry reactors predominate. The aforementioned light scattering issues are often neglected, making the comparison of rates difficult. In gas-phase applications, batch reactors are also usually applied (with the catalyst introduced as a loose powder on the bottom of a vessel),<sup>125</sup> since the catalytic rates usually do not warrant continuous operation. Some examples of reactors with coated catalyst exist, *e.g.* using optical fibre technology,<sup>126,127</sup> but these are still scarce. In the following, we evaluate the progress of improving rates in the photocatalytic reduction of CO<sub>2</sub> to produce fuels.

### Overview of photocatalysts for CO<sub>2</sub> reduction

Table S1 (see the ESI† and the references cited therein) compiles a selection of the studies reported in the literature since the 1980s until 2013,<sup>128–170</sup> including the applied process conditions (with as much details as possible). We have also constructed a figure based on these data, highlighting the limited progress that has been made over the years (Fig. 10). In contrast to what has been observed for the development of solar cell performance (see the well-known graph published by NREL<sup>123</sup>), there is not an apparent continuous improvement in the performance of photocatalysts in the reduction of CO<sub>2</sub> and H<sub>2</sub>O to fuels. Another observation is that most of the catalysts reported are based on TiO<sub>2</sub>, either supported or unsupported, and with and without catalytic promoters (noble metal particles). Commercial P25 is often used due to its availability and reproducibility. The disadvantage of these TiO<sub>2</sub>-based systems is that they are not photo-responsive to visible light. Hence, various efforts can be identified in Table S1† to synthesise and evaluate catalysts with visible light activity. This table also indicates the process conditions.

As aforementioned, both liquid and gas-phase studies have been conducted. In a recent review,<sup>171</sup> Garcia and coworkers already commented on an important issue of CO<sub>2</sub> reduction in the liquid phase. One of the problems associated with this methodology is that the standard reduction potential of H<sub>2</sub>O to form H<sub>2</sub> is considerably lower ( $E_{\text{red}}^{\circ} = 0 \text{ V}$ ) than the standard reduction potential of CO<sub>2</sub> to form CO<sub>2</sub><sup>-</sup> (1.9 V). Evaluation of the hydrogen quantities produced in CO<sub>2</sub> reduction conducted in the liquid phase is thus extremely important to validate the photon-, and overall catalyst efficiency. Making a valid quantitative comparison of catalytic performance in CO<sub>2</sub> reduction is furthermore difficult because of the following issues:

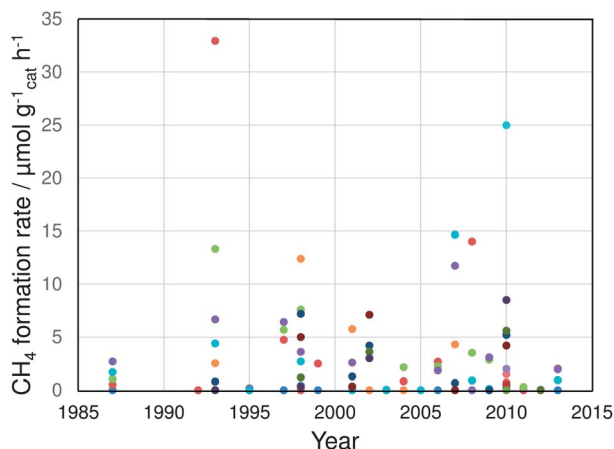


**Fig. 10** Representative data points reflecting the rates of photocatalytic CO<sub>2</sub> conversion to methane as a function of the year of study. Both liquid and gas phase operations are shown. Progress in enhancing rates is limited and a game changing material still needs to be developed. Selected rates are based on literature data compiled in Table S1.†<sup>128–170</sup>

1. As Table S1† shows, a large variety of illumination sources was used. This usually also impacts the reaction temperature, and thus the reported rates.<sup>136</sup> The effect of the diversity of the applied light sources and the reactor configurations is best illustrated by analysing the performance of the reference catalyst P25. Rates varying by one order of magnitude from 0.3 (ref. 141 and 149) to 4.7 μmol g<sub>cat</sub><sup>-1</sup> h<sup>-1</sup> (ref. 136) have been reported. A very peculiar activity has been recently reported for P25 by Wang *et al.*,<sup>170</sup> approaching 500 μmol g<sub>cat</sub><sup>-1</sup> h<sup>-1</sup>. We suspect that the last authors may have mislabelled the Y axis in their plots, *i.e.* μmol g<sub>cat</sub><sup>-1</sup> h<sup>-1</sup> should be used instead of mmol g<sub>cat</sub><sup>-1</sup> h<sup>-1</sup>.

2. Another relevant parameter to evaluate photocatalytic performance is the effectivity of the catalyst to convert light into chemical energy. Few papers report the quantum yield or efficiency, which requires measurement of the quantity of photons absorbed by the catalysts. Inaccuracy arises from how precisely the light intensity is probed. Similar issues arise when comparing materials in the photocatalytic production of hydrogen from water, as discussed by Maschmeyer *et al.*<sup>172,173</sup>

Still, the data in Table S1† provide trends and perspectives of photocatalytic CO<sub>2</sub> conversion in practice. Over the years, a few data points stand out (marked in the table), which require a more elaborated discussion.

### Isolated centres in zeolite matrices

First of all, the group of Anpo has reported extraordinary activities of zeolite and mesoporous supported TiO<sub>2</sub> based catalysts. As listed in Table S1,† the product yield was mostly determined based on the amount of titanium (μmol g<sub>Ti</sub><sup>-1</sup> h<sup>-1</sup>). Ikeue *et al.*<sup>140,141,174</sup> reported activities in the range of 200 μmol g<sub>Ti</sub><sup>-1</sup> h<sup>-1</sup> for zeolite supported Ti-centres. Hwang *et al.*<sup>149</sup> reported an activity of 100 μmol g<sub>Ti</sub><sup>-1</sup> h<sup>-1</sup> for SBA-15 supported TiO<sub>2</sub>. For silica-supported samples, like Ti-ZSM-5, Ti-MCM-41, Ti-MCM-48, Ti-SBA-15, and Ti-PS, low titania loadings ranging from 0.5 wt% to at most 10 wt% were applied, and quantification of rates per Ti quantity (based on ICP or XRF analyses) with

small error margins is difficult. Furthermore, since the product yields are very small, the role of impurities in the catalyst formulations should not be underestimated. Some of us have observed that pre-treatment in the presence of only steam is extremely important, since significant quantities of hydrocarbons can be formed in the absence of CO<sub>2</sub>.<sup>125,175</sup> Still, even considering some contribution of impurities, the reported activity of (usually) SiO<sub>2</sub> supported catalysts is up to 3 orders of magnitude higher *per* g<sub>Ti</sub> than that of P25 under similar conditions. Isolated centres consisting of tetrahedral sites are believed to be the active sites. The work of Frei and coworkers provides significant details on the mechanism of CO<sub>2</sub> reduction over these isolated centres, and variants of these to induce visible light sensitivity.<sup>176–179</sup> By using advanced IR spectroscopy it became clear that CO is an important intermediate in the conversion of CO<sub>2</sub>. Strikingly, these authors have not observed consecutive reactions under the conditions applied for the IR study, and the formation of hydrocarbons was not discussed.<sup>178,179</sup> Recently Yang *et al.*<sup>125</sup> have shown that formaldehyde is a very unstable potential intermediate to form hydrocarbons, and can be converted in the presence of the catalyst to products similar to those observed in the conversion of CO<sub>2</sub> and CO. It should be noted that formaldehyde strongly absorbs UV light, resulting in a rich photochemistry under the process conditions (UV illumination). As a final note, various IR studies have shown that carbonates in various forms can be formed and decomposed to CO and hydrocarbons upon light activation on semiconductor surfaces,<sup>160,175</sup> which will be discussed later. Carbonates have not been observed to play a role for the micro- and mesoporous silica supported catalysts.

### Semiconductors showing high apparent rates

Other rates with quantities significantly higher than usual were reported by Sasirekha *et al.*<sup>150</sup> for supported TiO<sub>2</sub> catalysts, with some possible effect of promotion by ruthenium. However, the light intensity in this study was considerably higher than reported by others, so temperature effects should not be ignored. Contributions of impurities cannot be excluded either. Very peculiar activities for CeO<sub>x</sub> containing TiO<sub>2</sub> formulations have been reported by Wang *et al.*<sup>170</sup> We believe these numbers are not to be taken seriously, since the activity reported for P25 was also way beyond the ordinary, approaching 500 μmol g<sub>cat</sub><sup>-1</sup> h<sup>-1</sup>. Still, the reported beneficial effect of CeO<sub>x</sub> addition shifting the absorption spectrum of composites more to the visible merits further investigation.

### Co-catalysts

Without discussing the rates provided in Table S1† in too much detail, another trend is obvious: adding co-catalysts in the form of small quantities of noble metals enhances the values observed. Ishitani *et al.*<sup>132</sup> have reported an order of magnitude increase in rates by adding noble metals and Cu. The order in observed rates was Pd > Rh > Pt > Au > Cu, with Ru showing the least effect. The low response to rate by adding Ru is remarkable, since other researchers have observed significant improvement by adding Ru(O<sub>2</sub>) to catalyst formulations. RuO<sub>2</sub>

needs to be formed in the preparation procedure, and rather than a promoting function by physical improvement of the lifetime of photo-excited states, the promotion of RuO<sub>2</sub> is ascribed to introducing a high water oxidation activity. RuO<sub>2</sub> was also found to significantly enhance the rate of mesoporous ZnGa<sub>2</sub>O<sub>4</sub>.<sup>164</sup> The beneficial effect of adding nanosized metal particles as co-catalysts is usually ascribed to the improved separation of electron-hole pairs generated upon photo-excitation. Pt was also found to promote the activity of composites like CuGaAlO<sub>4</sub><sup>169</sup> and TiO<sub>2</sub> nanotubes.<sup>159</sup> Other oxides such as IrO<sub>x</sub>, MnO<sub>x</sub> and Co<sub>3</sub>O<sub>4</sub> have been reported to enhance water oxidation rates, when supported on semiconductor surfaces, and applied in the overall splitting of water to hydrogen and oxygen.<sup>180–182</sup>

### Copper promoted systems

One very interesting system that has also been extensively discussed in the literature is copper promoted TiO<sub>2</sub>. The findings reported for this material have recently been reviewed by Garcia *et al.*<sup>171</sup> To summarise, the preparation of the Cu-promoted TiO<sub>2</sub> catalysts largely affects the performance. Impregnation leads to less active materials as compared to compositions prepared by sol-gel methods. Methanol forms a major product.<sup>171</sup> Significant amounts of methanol have also been observed in an optical fibre reactor.<sup>127,183</sup> Yang *et al.*<sup>175</sup> recently reported the formation of large quantities of CO adsorbed on Cu<sup>+</sup> sites, and evaluated this to be a true product of CO<sub>2</sub> reduction by using <sup>13</sup>C-labeled CO<sub>2</sub>, whereas significant quantities of the CO product were observed to result from water induced contaminant oxidation. Recently, others have also observed the formation of large quantities of CO with a SiO<sub>2</sub> supported Cu/TiO<sub>2</sub> system.<sup>162</sup> The catalyst was found to deactivate over time. While changes in the oxidation state of copper have been argued to be detrimental to the performance (it is proposed that Cu<sup>0</sup> is formed from more active Cu<sup>I</sup> sites), an issue of carbon contamination might also explain the data: contaminants will be depleted after a certain period of time, lowering the apparent formation of CO and hydrocarbon products. In conclusion, certainly Cu-containing TiO<sub>2</sub> catalysts are worth studying, including the role of the oxidation state and stability. However, as always, care should be taken when assigning hydrocarbon products to CO<sub>2</sub> reduction, that is, to exclude contributions of carbon contaminants.

### The relevance of adsorption of CO<sub>2</sub>

Dissolution of CO<sub>2</sub> in water initially results in the formation of carbonates and bicarbonates, and the question arises if it is feasible to directly reduce these species upon illumination. Chandrasekaran *et al.*<sup>184</sup> first demonstrated the photochemical reduction of carbonates into formaldehyde over TiO<sub>2</sub> powder. The yield of formaldehyde was found to be independent of the concentration of Na<sub>2</sub>CO<sub>3(aq)</sub> (from 0.01 to 1 M). Raphael *et al.*<sup>185</sup> reported the activity of platinised titania suspended in a Na<sub>2</sub>CO<sub>3</sub> solution under UV/visible light irradiation. Their results showed the formation of CH<sub>3</sub>OH, 'C', HCHO and HCOO<sup>-</sup> ions in the absence of CO<sub>2</sub>, which was quantified by spectro-photometrical methods. While aqueous phase carbonate reduction has been

reported, understanding the role of surface adsorbed carbonates in the gas-phase conversion of CO<sub>2</sub> is also extremely relevant for a configuration in which CO<sub>2</sub> is accumulated in the dark on the surface of an inorganic semiconductor, and converted during exposure to sunlight. Carbonates have been demonstrated to be easily formed on the surface of TiO<sub>2</sub> by IR spectroscopy, and have been proposed as intermediates in the photocatalytic decomposition of CO<sub>2</sub>. Some aspects of the mechanism of carbonate decomposition on TiO<sub>2</sub> surfaces have been addressed.<sup>148,185,186</sup> There is no agreement on this mechanism, however. In particular, Chandrasekaran *et al.*<sup>184</sup> suggested that the carbonate ion can be considered as a hole acceptor, and is oxidised, as demonstrated by laser flash pyrolysis experiments. The neutral carbonate radical is then proposed to decompose into CO and O<sub>2</sub>. The electron is either scavenged by oxygen or involved in the reduction of protons to hydrogen, eventually leading to the catalytic reduction of CO to form the product formaldehyde. In contrast to this mechanism, Raphael and Malati,<sup>185,186</sup> and later Ku *et al.*<sup>148</sup> argued that carbonate is the electron acceptor, and proposed a route in which carbonate is first reduced to formate, and subsequently to formaldehyde and methanol. Water is oxidised by holes leading to the evolution of O<sub>2</sub>. An argument against the oxidation of carbonate used by Raphael *et al.*<sup>179</sup> and Malati *et al.*<sup>185,186</sup> is the incompatibility of this mechanism with the formation of formaldehyde. Recently, Dimitrijevic *et al.*<sup>187</sup> used EPR spectroscopy to study the reduction of CO<sub>2</sub> to CH<sub>4</sub> on TiO<sub>2</sub> surfaces in the presence of light. Important steps in the mechanism were also discussed. A mechanism involving a two-electron, one-proton reaction was confirmed by first-principles calculations. It should be mentioned that the nature of the site on which the carbonate is adsorbed possibly affects the pathway: experiments applying metal deposition have demonstrated that holes and electrons might preferentially accumulate on specific crystal facets.<sup>188</sup> *In situ* IR studies are needed to shed more light on the mechanistic routes.

### C<sub>3</sub>N<sub>4</sub> based catalysts

Many alternative doped oxides, sulfides, and materials known from the solar cell industry have been tested for the photocatalytic decomposition of CO<sub>2</sub>. One of the materials we envision as promising is γ-C<sub>3</sub>N<sub>4</sub>, since it is composed of elements which are widely available in nature, and it can be easily formed by thermal treatment of (cheap) precursor molecules. γ-C<sub>3</sub>N<sub>4</sub> based catalysts are reportedly effective in the overall water splitting reaction, and their photocatalytic properties have been recently reviewed by Zheng *et al.*<sup>189</sup> The band gap positions of these materials are quite favourable for the absorption of light in the near UV and visible range, whereas the potential of the generated electrons in the conduction band is sufficient to drive CO<sub>2</sub> reduction reactions. In water splitting experiments using sacrificial agents (triethanol amine for hydrogen evolution and silver nitrate for oxygen evolution), considerable rates have been observed. Surprisingly, to the best of our knowledge these materials have not yet been evaluated in the reduction of CO<sub>2</sub>, while another property of these materials appears to be

beneficial: nitrogen containing hydrocarbons have very good CO<sub>2</sub> adsorption properties, and we expect that  $\gamma$ -C<sub>3</sub>N<sub>4</sub> will have a reasonable CO<sub>2</sub> adsorption capacity. Future studies will reveal the significance of  $\gamma$ -C<sub>3</sub>N<sub>4</sub> in photocatalytic CO<sub>2</sub> conversion.

### Conclusions on heterogeneous photocatalysis

Based on the above discussion regarding the highest reported activities, one can conclude that game-changing rates have not yet been achieved in the direct photocatalytic production of hydrocarbons from CO<sub>2</sub> and H<sub>2</sub>O. Yang *et al.* attempted to convert the reported rates into a turnover frequency of the materials.<sup>125</sup> Even for Ti-SBA-15, the turnover frequency is only  $8.6 \times 10^{-4} \text{ h}^{-1}$ . Such small turnover frequencies are far from those required for an efficient catalytic process, and an efficiency improvement of at least 3 orders of magnitude is needed to bring artificial photosynthesis closer to reality. Moreover, the apparent quantum yield (AQY) is 0.01%. This means at best only a minute fraction of the photons is used effectively for the reaction. The recent attempts of the group of Frei<sup>190</sup> using visible light sensitive sites connected to a nanoparticle oxide water oxidation catalyst appear to be an interesting way forward to improve the quantum yield and use solar radiance more effectively.

### Fundamental basis for rational design of CO<sub>2</sub> conversion catalysts

Quantum chemical methods and their use in elucidating fundamental aspects of catalytic performance in various CO<sub>2</sub> transformations have rapidly evolved in recent decades. In particular, owing to its relatively low computational cost combined with its appreciable accuracy, Density Functional Theory (DFT) has been routinely applied across all science and engineering disciplines for predicting the molecular and crystalline structures as well as the bulk and surface properties of inorganic, organic, and organometallic compounds.<sup>191–196</sup> Here, we will focus on elucidating methods and predictions of active catalysts for CO<sub>2</sub> activation using: (i) thermal energy to overcome the activation barrier, (ii) electrochemistry as a source of readily available electrons, and (iii) photocatalytic activation.

### Heterogeneous CO<sub>2</sub> hydrogenation to methanol

As mentioned in the “Formation of oxygenates from CO<sub>2</sub>” section, supported Cu-containing materials are industrially attractive catalysts for the conversion of CO<sub>2</sub> to methanol. The unique catalytic property of Cu is probably related to its ability to stabilise surface formate (HCOO) or hydrocarboxyl (COOH) species.<sup>66,78,79</sup> This property is increased over step sites and in the presence of ZnO.<sup>66</sup> This knowledge opens the possibility to design more active and selective catalysts.

Computational DFT-based techniques promise an unprecedented capability to explore alternative elemental compositions to the conventional catalysts without performing tedious experimental synthesis and evaluation. For example, the selectivity of CO<sub>2</sub> hydrogenation on Pd/ $\gamma$ -Al<sub>2</sub>O<sub>3</sub> was predicted to depend on competing reaction pathways leading to CO and

HCOO species, which can be regarded as intermediates in the formation of methane and methanol, respectively.<sup>197,198</sup> These DFT data thus imply that CO<sub>2</sub> methanation will be favoured if support materials have a low water affinity. In contrast, methanol would be formed if controllable hydroxylation of the support surface was achieved. The latter conclusion was substantiated by DFT calculations of the hydrogenation of CO<sub>2</sub> on Co/Cu clusters supported on a hydroxylated  $\gamma$ -Al<sub>2</sub>O<sub>3</sub>.<sup>199,200</sup> Furthermore, incorporation of Cu atoms into Co clusters resulted in a 0.24 eV decrease in activation energy towards HCOO formation. A negative effect of surface hydroxylation is the weaker interaction between the  $\gamma$ -Al<sub>2</sub>O<sub>3</sub> support and the Pd clusters, which may decrease the palladium dispersion and hence total activity, and catalyst stability and lifetime.<sup>197</sup>

Other unconventional catalysts computationally explored for the hydrogenation of CO<sub>2</sub> to methanol were Au/TiC,<sup>77</sup> Cu/TiC,<sup>77</sup> and Co/WC.<sup>201</sup> Cu and Au nanoparticles were shown to undergo a charge polarization on a TiC support to become active catalytic centres for the conversion of CO<sub>2</sub> to CH<sub>3</sub>OH. This can be regarded as a new approach in the design of methanol synthesis catalysts; conventional catalysts are based on achieving strong interactions between Cu and ZnO on an Al<sub>2</sub>O<sub>3</sub> support of high surface area. Metal carbide supports, on the other hand, are known as very stable compounds that also induce the polarisation of *ad*-metals (metal atoms that sit on top of the surface), thus facilitating methanol synthesis.

In addition to copper and palladium catalysts, Mo<sub>6</sub>S<sub>8</sub> clusters were shown *via* DFT studies to selectively convert CO<sub>2</sub> and H<sub>2</sub> into CH<sub>3</sub>OH.<sup>198</sup> Due to the lower S/Mo ratio than in bulk MoS<sub>2</sub>, Mo<sub>6</sub>S<sub>8</sub> was shown to facilitate the dissociation of adsorbed H<sub>2</sub> by forming S–H bonds, thus increasing the selectivity towards methanol.<sup>202</sup> Mo atoms were involved in the binding of CO<sub>2</sub> as well as in the formation of carbon intermediates. The proposed reaction pathway involved the RWGS reaction with the formation of CO followed by its hydrogenation *via* HCO into CH<sub>3</sub>OH. HCO formation was found to be rate limiting with an activation barrier of 1 eV, even smaller than the comparable energy on the surface steps of Cu nanoparticles. These sub-stoichiometric metal sulphide nanoclusters suppress hydrocarbon formation, albeit at the expense of activity. The use of nanoparticulate MoS<sub>2</sub> for the synthesis of alcohols from syngas has been demonstrated by PowerEnerCat, Inc.<sup>203</sup> A small amount of sulphur in the feed was essential to ensure sub-stoichiometric conditions, similar to the CO<sub>2</sub> activation process on the Mo<sub>6</sub>S<sub>8</sub> catalyst discussed here. Another transition metal sulphide, Fe<sub>2</sub>S<sub>2</sub>, clusters have also been reported to form methanol *via* a barrier-free, thermodynamically favourable pathway showing the potential of metal sulphide nanoparticles and clusters in selective CO<sub>2</sub> hydrogenation.<sup>204</sup> A possible interplay between particle size and stoichiometry needs to be explored computationally in more detail.

Electrocatalytic CO<sub>2</sub> activation on metal surfaces has a well-established computational basis, recently developed by Nørskov *et al.*<sup>205–207</sup> Briefly, this method is based on calculating the binding energies ( $E_B$ ) of adsorbate molecules, which are a basis for estimating the corresponding chemical potentials. The latter are used to calculate a limiting potential  $U_L$  (eqn (9)), *i.e.*



the potential at which each elementary step of a reaction becomes exergonic.

$$U_L = \frac{\mu[\text{B}^*] - \mu[\text{A}^*] - \mu[\text{H}^+ - \text{e}^-](U = 0V_{\text{RHE}})}{e^-} = -\frac{\Delta G_{\text{elem}}^{0V}}{e^-}, \quad (9)$$

where \* signifies adsorbed species,  $\mu[\text{A}, \text{B}]$  is the chemical potential of any generic surface species found from a standard statistical mechanics treatment of the calculated binding energies ( $E_{\text{B}}$ ) of these adsorbed species,  $\Delta G_{\text{elem}}$  is the free energy change of the elementary reaction and  $e$  is the (positive) charge of an electron and the chemical potential of the proton.

The calculated potentials then provide the overpotential necessary for the electrocatalytic transformation of  $\text{CO}_2$ , thus quantitatively establishing the reactivity of a series of electrocatalysts. Systematic activity trends have recently been calculated and compared using this method for the facets of late transition metals of face centred cubic (fcc) structure, which are routinely used as electrocatalysts.<sup>207</sup> A measure of activity was suggested to be the difference between  $U_L$  and the equilibrium potential, representing the overpotential for the elementary reactions shown in Fig. 11.

Based on these values for the metals analysed, it was concluded that the protonation of adsorbed CO species to CHO was an important rate-limiting step in the mechanism of carbon intermediate transformations. Cu showed the lowest calculated overpotential (top of the “volcano plot” in Fig. 11) for this step, indicating its superior performance in electrocatalytic  $\text{CO}_2$  conversion to form hydrocarbons. This predicted rate-limiting step agrees well with the common phenomena of catalyst CO poisoning due to its strong binding on other metals, and can explain the high values of the calculated overpotentials. Using the same computational approach to compare different copper facets, the lowest limiting potential for  $\text{CO}_2$  electrocatalytic reduction into  $\text{CH}_4$  was found for the fcc Cu (211) surface, that is the formation of hydrocarbons proceeds more easily on the stepped surfaces of Cu than on other facets.<sup>206</sup> It is worth noting that a similar order of activity was predicted for the hydrogenation of  $\text{CO}_2$  to methanol over Cu(211) and Cu(111). Therefore,

it can be suggested that irrespective of the mode of  $\text{CO}_2$  activation, defect-rich Cu surfaces will show high catalytic activity.

An important conclusion drawn for the electrochemical reduction of  $\text{CO}_2$  to  $\text{CH}_4$  is that a prospective material must be found that binds to CHO species more strongly than CO, *e.g.* with greater affinity towards the oxygen atom.<sup>207</sup> This is due to the fact that gaseous CO is more stable than adsorbed, resulting in the liberation rather than the protonation of CO molecules. The primary approaches here would be through the application of a controlled surface doping or co-binding with other adsorbed species that donate electron density to carbon or withdraw electron density from the oxygen in CHO, thus increasing the degree of  $\text{sp}^2$  character of the adsorbed CHO, as well as its binding energy. The general difficulty here is in discerning coupled electronic and structural effects of surface dopants with the goal of changing the reduction potential of  $\text{CO}_2$ .

### Co-catalysts

The use of pyridine as a co-catalyst in the photoelectrochemical reduction of  $\text{CO}_2$  to  $\text{CH}_3\text{OH}$ <sup>112</sup> over a p-GaP semiconductor electrode has spurred a series of theoretical studies.<sup>208–212</sup> A pyridinyl radical has been proposed to be involved in a one electron step as a strong reductant to form a carbamate intermediate, which can then yield formic acid, formaldehyde, and finally methanol.<sup>208</sup>

Modifications to the thermodynamic cycle have also been made to uncover the systematic trends in the  $\text{p}K_{\text{a}}$  of substituted pyridines with electron withdrawing ( $\text{Cl}^-$  or  $\text{CHO}^-$ ) or electron donating (Me,  $\text{NH}_2^-$ ) groups, which decrease or increase the  $\text{p}K_{\text{a}}$ , respectively.<sup>212</sup> Such a procedure permits the intelligent design of pyridine-based  $\text{CO}_2$  activation catalysts. However, calculated  $K_{\text{a}}$  values of such substituted pyridinyl species were 10 to 20 times higher than their pyridinium counterparts, making them poor proton donors to  $\text{CO}_2$ . Instead, the recombination of two pyridinyl-containing units into pyridines and formic acid was shown to be thermochemically favourable, depending on the reaction (reaction steps 12, 17 and 22 in

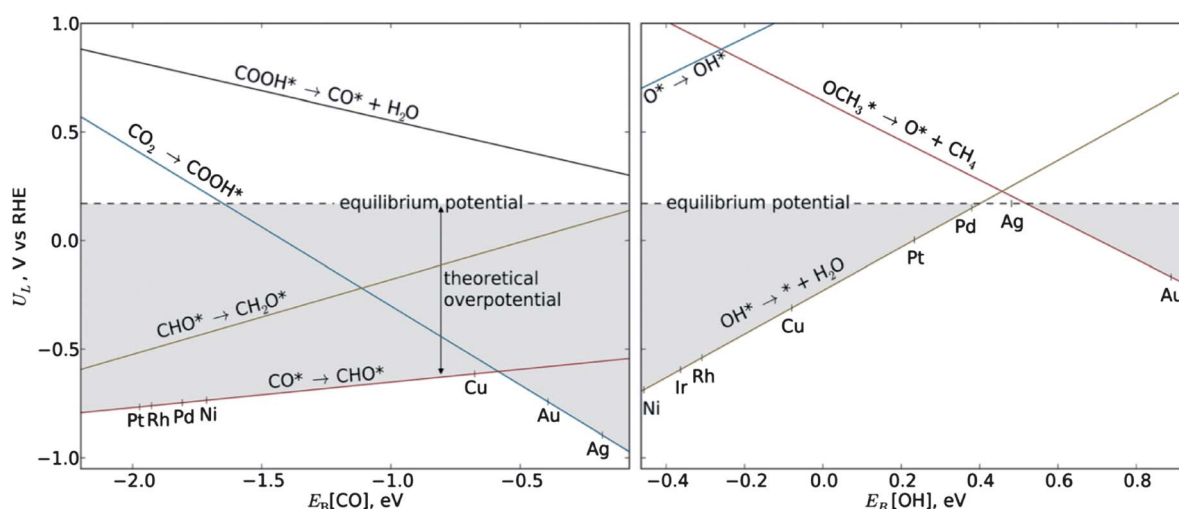


Fig. 11 Calculated limiting potentials for elementary steps upon  $\text{CO}_2$  hydrogenation to  $\text{CH}_4$  on fcc transition metal electrocatalysts (from ref. 207).

| Rxn Step | Reaction | $\Delta G$ kcal mol <sup>-1</sup> |
|----------|----------|-----------------------------------|
| 5        |          | 7.46                              |
| 12       |          | -50.2                             |
| 16       |          | 0.292                             |
| 17       |          | -38.4                             |
| 21       |          | 1.29                              |
| 22       |          | -62.5                             |

Fig. 12 Reaction pathways and their calculated free energies in the reduction of CO<sub>2</sub> to methanol. Adapted from ref. 209.

Fig. 12).<sup>209</sup> Such thermodynamic efficiency implies that electron-storage molecules having the inherent ability to coordinate hydrogen atoms can act as efficient intermediates in CO<sub>2</sub> activation.

To design the most effective organic system for CO<sub>2</sub> activation, computational studies need to be performed with a series of  $\pi$ -bonded cyclic hydrocarbons to establish the electron donating capacities between the nitrogen containing ring and the CO<sub>2</sub> molecule *via* an inner sphere coordination mechanism. Another challenge is to design a selective electrocatalytic process, as many-electron reactions are usually non-selective. Formic acid, formaldehyde and methanol were all observed as intermediates or final products at some point of the reaction, while the production of H<sub>2</sub> considerably reduced the Faradaic efficiency.

### Photocatalysis and photolysis

**Metal oxide semiconductors.** Most of the theoretical studies in the development of photocatalysts focused on modelling the solid state band structure and the changes caused by the formation of vacancies due to substitutional doping.<sup>213–215</sup> Further, accurate prediction of the band edge positions for wide bandgap semiconductors to be able to drive the photocatalytic reduction of CO<sub>2</sub> has been achieved.<sup>216,217</sup> The predicting capability of DFT can also serve to describe subtle electronic effects that notably change the activity of photocatalytic CO<sub>2</sub> reduction. Band flatness arguments can be used to describe the kinetic energy, hence the mobility of the charge carrier, as well as (de) localization of the electronic bands.<sup>215,217</sup> Since the potential for the photocatalytic reduction of CO<sub>2</sub> into hydrocarbons is close

to that of H<sub>2</sub> evolution,<sup>9</sup> the vast knowledge acquired by evaluating materials for their band positions is of value to predict active CO<sub>2</sub> reduction photocatalysts. For example, modifications of valence band of semiconductors to absorb in a wider range of the solar spectrum can be applied as a tool for predicting which dopants would decrease it, but not necessarily for forecasting enhanced photoreactivity towards CO<sub>2</sub>. Only the energetically (un)favourable photocatalyst band alignment with CO<sub>2</sub> reduction potential can be predicted using this method whereas kinetics and thermodynamics require standard surface-adsorbate interaction calculations. To this point, the inherent affinity of Cu, most likely in the form of Cu<sub>2</sub>O, towards CO<sub>2</sub> can be explored to devise efficient photocatalysts by performing DFT band position screening of alternative semiconductor materials, including those not commonly applied. Nitrides, carbides, phosphides or silicides have bandgap magnitudes capable of absorbing UV/visible light, and might thus be of use.<sup>218</sup> This recently has been attempted when combining Cu<sub>2</sub>O and SiC nanoparticles to photocatalytically produce CH<sub>3</sub>OH from CO<sub>2</sub>.<sup>219</sup> The low methanol yields reported (191  $\mu$ mol per g catalyst) are typical for the photocatalytic processes involved; efficiency needs to be improved by several orders of magnitude to bring the photocatalytic activation of CO<sub>2</sub> within practical usability.

**Organic molecules as renewable or sacrificial hydrogen donors.** Stable metal oxide semiconductors, such as TiO<sub>2</sub>, have been core materials of interest in photocatalysis for many decades. They usually are doped with cations or anions to modify either their electron or hole conductive properties, or the magnitude of the bandgap to absorb visible light. A recent, conceptually very different approach is using purely organic solar light absorbing materials.<sup>220,221</sup> That comes with an added benefit that, somewhat auspiciously, organic molecules mostly cannot operate under UV light conditions due to their stability; thus, visible light organic molecules need to be used which is favourable for any practical purpose. A very elegant approach was reported by Carpenter and Rose<sup>221</sup> where the B3LYP hybrid functional combined with 6-31+G(d, p) basis sets and IEFPCM simulated acetonitrile solvent were used to design an organic compound for the conversion of CO<sub>2</sub> to formic acid circumventing the generation of CO<sub>2</sub><sup>-</sup>. Instead, hydride generating organic molecules based on substituted naphthalene were devised, which after the initial photon absorption undergo series of elementary intramolecular reaction steps, involving intersystem crossing from S1 to T3, enabling hydride transfer to CO<sub>2</sub> to form formic acid. A hydrogenation step has to be involved to regenerate the organic molecule, thus being one step short of fully renewable.

Intricate methods to describe the electronic structure of the organic molecules in the excited state have been devised (TDDFT, CIS, SAC-CI, CC2, CC3, EOM-CCSD, MRCI, CASSCF),<sup>222</sup> which simply are either not accurate or cannot be sustained computationally for large transition metals. However, homogeneous processes can be described efficiently. With this in mind, other light absorbing organic molecules, such as H<sub>2</sub>S or CH<sub>3</sub>SH, prevalent as byproducts in natural gas, have been modelled to act as a source of hydrogen atoms in the excited

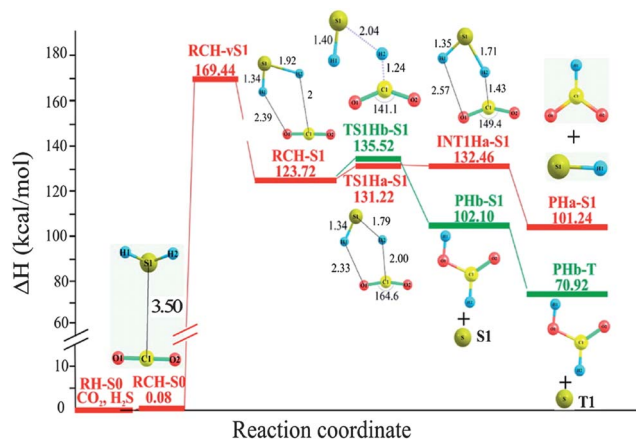


**Fig. 13** CR-EOMCC(2,3)/6-311+G(2df, 2p)//CAM-B3LYP/6-311+G(2df, 2p) reaction energy diagram of  $\text{CO}_2$  and  $\text{H}_2\text{S}$  reactions optimized on the S1 surface. All enthalpies are referenced to those of separated  $\text{CO}_2$  and  $\text{H}_2\text{S}$  optimized in the S0 state. Reaction path A (C–S bond formation mechanism) is shown in red, whereas path B (H–S bond formation mechanism) is shown in green. Adapted from ref. 223.

state. The calculated values of the absorbed wavelengths were 205 and 231 nm, respectively.<sup>223</sup> This effort is substantiated by the fact that the bond dissociation energy of S–H in  $\text{H}_2\text{S}$  is  $\sim 120 \text{ kJ mol}^{-1}$  smaller than that of O–H in  $\text{H}_2\text{O}$ , making it easier to break electro- or photochemically. Electrochemical hydrogen transfer from a thiol group to  $\text{CO}_2^-$  to form formic acid was modelled at ground state using the B3LYP and M06X density functionals applying an explicitly solvated cluster model.<sup>224</sup> Furthermore, excited state DFT simulations were performed to investigate whether organic sulphur species can be facile hydrogen atom donors.<sup>223</sup> Geometry optimization using long range corrected CAM-B3LYP density functional showed that the SH bond, 1.34 Å in the ground state in both  $\text{H}_2\text{S}$  and  $\text{CH}_3\text{SH}$ , was elongated to 1.94 and 1.85 Å in the 1<sup>st</sup> excited state for  $\text{H}_2\text{S}$  and  $\text{CH}_3\text{SH}$ , respectively, indicating formation of a neutral diradical. This very reactive hydrogen atom can react *via* a low energy transition state with the carbon atoms in  $\text{CO}_2$  forming formate species as shown in Fig. 13, a reaction which is unavailable *via* ground state chemistry.

This mechanism utilises the photolytic  $n-\sigma^*$  excitation of the donor molecule. This shows that once excited, mixtures of possible hydrogen atom donors react with  $\text{CO}_2$  to activate the latter exergonically. Besides the above mentioned  $\text{H}_2\text{S}$  and  $\text{CH}_3\text{SH}$ , compounds of practical importance to activate  $\text{CO}_2$  photolytically would be alcohols, such as  $\text{CH}_3\text{OH}$  or isopropyl alcohol, but not organic acids due to the  $n-\pi^*$  transition of the carboxylic group.

## Comparison of different approaches for $\text{CO}_2$ functionalisation

Irrespective of the way  $\text{CO}_2$  is converted to value-added products, the profitability of the overall process depends not only on the value of the final products, but also on the energy and consumables required for process operation. Therefore, we start with an analysis of the overall energy balance of catalytic  $\text{CO}_2$

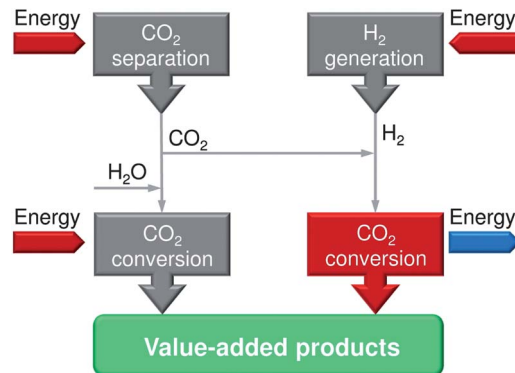


**Fig. 14** Simplified energy diagram of conversion of  $\text{CO}_2$  to value-added products. Red and blue arrows indicate energy consumption and release, respectively.

hydrogenation, as well as electron- and photon-assisted approaches. Fig. 14 shows a simplified energy diagram. Initially, and very importantly,  $\text{CO}_2$  must be separated from flue gases or air. Various methods can be used.<sup>50</sup> The best available technique at present is to absorb the  $\text{CO}_2$  present in the flue gas in an amine solution. The amine from the scrubber is then heated by steam to release high-purity  $\text{CO}_2$ , and the  $\text{CO}_2$ -free amine is reused. According to ref. 225, *ca.* 53 and  $158 \text{ kJ mol}^{-1}$  ( $\text{CO}_2$ ) are required for the separation of  $\text{CO}_2$  from feeds containing 11 vol % and 300 ppmv  $\text{CO}_2$ , respectively. For the electro- or photocatalytic conversion of  $\text{CO}_2$ , additional energy input is required, which is obviously the solar energy that one likes to directly (photocatalysis), or indirectly (electrocatalysis) store in the process. We consider the formation of methane, methanol and formic acid, *i.e.* typical products reported in the literature. The respective chemical equations and enthalpies are given in Table 2. It is obvious that methane formation requires the highest amount of energy. However, even for this case, the energy for  $\text{CO}_2$  separation amounts to 6–17% of the overall energy required. This value increases up to 60% when  $\text{CO}_2$  is converted to formic acid, the formation of which requires the lowest amount of energy. Thus, further developments in  $\text{CO}_2$  capturing technologies are necessary to improve the overall energy balance of  $\text{CO}_2$  conversion to useful chemicals.

Compared to photo- or electrocatalytic  $\text{CO}_2$  transformations,  $\text{CO}_2$  hydrogenation is generally an exothermic process. The most representative reactions and their enthalpies are summarised in Table 2; reaction 7 represents  $\text{CO}_2$  conversion to higher hydrocarbons (FT-products). The  $\text{CO}_2$  conversion to  $\text{CH}_4$

**Table 2**  $\text{CO}_2$  conversion to various chemicals and the corresponding enthalpies

| Nr. | Reaction   | $\Delta H_{298\text{K}}^0$<br>$\text{kJ mol}^{-1}$ ( $\text{CO}_2$ ) |
|-----|--|--|
| 1   | $\text{CO}_2(\text{g}) + 2\text{H}_2\text{O}(\text{l}) \rightarrow \text{CH}_4(\text{g}) + 2\text{O}_2(\text{g})$            | 890.9  |
| 2   | $\text{CO}_2(\text{g}) + 2\text{H}_2\text{O}(\text{l}) \rightarrow \text{CH}_3\text{OH}(\text{l}) + 1.5\text{O}_2(\text{g})$ | 726.7  |
| 3   | $\text{CO}_2(\text{g}) + \text{H}_2\text{O}(\text{l}) \rightarrow \text{CHOOH}(\text{l}) + 0.5\text{O}_2(\text{g})$          | 255.0  |
| 4   | $\text{CO}_2(\text{g}) + 4\text{H}_2(\text{g}) \rightarrow \text{CH}_4(\text{g}) + 2\text{H}_2\text{O}(\text{g})$            | −165.1   |
| 5   | $\text{CO}_2(\text{g}) + 3\text{H}_2(\text{g}) \rightarrow \text{CH}_3\text{OH}(\text{g}) + \text{H}_2\text{O}(\text{g})$    | −49.7  |
| 6   | $\text{CO}_2(\text{g}) + \text{H}_2(\text{g}) \rightarrow \text{CHOOH}(\text{g})$  | 14.9   |
| 7   | $\text{CO}_2(\text{g}) + 3\text{H}_2(\text{g}) \rightarrow -\text{CH}_2-(\text{g}) + 2\text{H}_2\text{O}(\text{g})$          | −110.8   |
| 8   | $\text{CO}_2(\text{g}) \rightarrow \text{CO}(\text{g}) + 0.5\text{O}_2(\text{g})$  | 283.2  |

leads to the highest energy release. However, one also has to take into account the energy required for H<sub>2</sub> production from renewable sources. For example, high-temperature (1073 K) water (steam) electrolysis requires 248.5 kJ mol<sup>-1</sup> (H<sub>2</sub>O). It is worth mentioning that modern water electrolyzers operate with significantly higher energy efficiencies than those reported for various technologies using direct electro- or photocatalytic CO<sub>2</sub> conversions. As a consequence, the latter must be significantly improved in order to compete with catalytic CO<sub>2</sub> hydrogenation in terms of energy consumption. To this end, novel electrodes and catalysts are required. Another drawback of electro- or photocatalytic CO<sub>2</sub> conversion processes is the low solubility of CO<sub>2</sub> in water, which leads to mass transport limitation. This problem can be overcome by: (i) using gas diffusion electrodes, (ii) organic solvents or (iii) operating at elevated pressures or (iv) application of supercritical fluid. Some process options used in practice are discussed below.

From an energetic viewpoint, formic acid requires the lowest amount of energy (Table 2), which is highly attractive for possible commercial application. Actually, the University of British Columbia's Clean Energy Research Center headed by Professor Colin Oloman developed a technology for the electrocatalytic conversion of CO<sub>2</sub> to formic acid. This technology was acquired by Mantra Energy<sup>226</sup> and is now called ERC (Electro Reduction of Carbon dioxide). This company is going to start demonstration projects in North America and in Asia in order to derive data for process economics. Since the global market of formic acid is relatively small it must also be demonstrated that the ERC process will strongly contribute to reducing total CO<sub>2</sub> emissions. If formic acid will be used as an energy carrier (large-volume consumption), the CO<sub>2</sub> emissions cannot be reduced unless CO<sub>2</sub> is also recycled since CO<sub>2</sub> will be formed upon the decomposition of formic acid. Moreover, the energy density of formic acid is significantly lower than that of conventionally used fuels and methanol.

Given the above arguments and the increasing demand for methanol, a CO<sub>2</sub>-based methanol technology is highly relevant. The energy requirements are significantly higher than for the production of formic acid. As mentioned in the "Formation of oxygenates from CO<sub>2</sub>" section, methanol formation *via* catalytic CO<sub>2</sub> hydrogenation has already been industrially implemented by Carbon Recycling International (CRI) in Iceland.<sup>53</sup> However, compared to commercial CO-based methanol synthesis, the alternative process requires a higher amount of H<sub>2</sub> and suffers from a lower productivity. This drawback can be overcome by using CO<sub>2</sub>-CO mixtures. In fact, modern methanol plants co-feed CO<sub>2</sub> as a promoter to the CO-H<sub>2</sub> feed. Owing to the low-energy demand for the formation of CO from CO<sub>2</sub> (reaction 8 in Table 2), an interesting process option is to combine electrocatalytic CO<sub>2</sub> conversion to CO (Fig. 15) with catalytic methanol synthesis. The former process will provide a mixture of CO and CO<sub>2</sub>, which can be directly fed to a methanol synthesis reactor without expensive separation steps. The degree of CO<sub>2</sub> conversion in the first reactor will determine the amount of hydrogen required for methanol production. The above approach can also be applied for FT synthesis. Since both these hydrogenation processes require high pressures, energy is required to build up

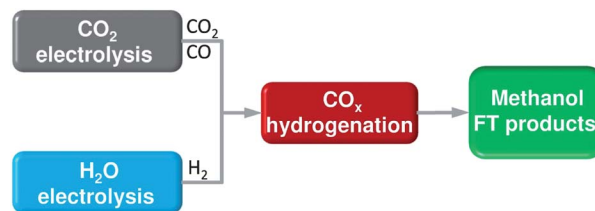


Fig. 15 Scheme for methanol formation *via* CO<sub>2</sub> and CO hydrogenation.

pressure after electrolysis of H<sub>2</sub>O and CO<sub>2</sub> or to perform electrolysis at high pressures. A deeper analysis is necessary to ascertain optimal operation conditions, *e.g.* CO/CO<sub>2</sub> ratio, reaction temperature, total pressures of hydrogenation and electrolysis processes.

In summary, technologies based on catalytic CO<sub>2</sub> hydrogenation to useful chemicals appear to be more industrially attractive than electro- or photocatalytic CO<sub>2</sub> transformations. This is mainly due to the low energy efficiency and productivity of the latter processes. All the above technologies rely on efficient CO<sub>2</sub> capture, purification, and delivery.

## Conclusions and outlook

The present study has analysed the current status of the conversion of carbon dioxide to chemicals by catalytic hydrogenation, photo- and electrocatalytic processes. The main focus was put on the catalytic aspects. Some reaction engineering concepts have also been discussed. It has been proven on different developmental levels that carbon dioxide is a promising and powerful alternative to produce CO<sub>2</sub>-neutral renewable fuels and commodity chemicals. The catalytic hydrogenation of CO<sub>2</sub> to methanol and methane is now at a commercial scale. These technologies are, however, viable because of the presence of (i) CO<sub>2</sub> streams from local biomass or power plants and (ii) H<sub>2</sub> produced *via* water electrolysis using inexpensive renewable power sources. Their economy will be significantly improved when novel cost- and energy-efficient methods for providing large amounts of pure CO<sub>2</sub> are developed. In addition, more active catalysts are required since CO<sub>2</sub> is a very stable molecule that is reflected in low catalyst productivity when comparing with classical processes operating with CO. This is also valid for CO<sub>2</sub>-based Fischer-Tropsch synthesis, which has high potential for recovering large amounts of CO<sub>2</sub> to synthetic fuels.

Significant technical and catalytic advances are still required for the large-scale use of electro- and photocatalytic routes for CO<sub>2</sub> conversion into fuels and chemicals due to their low energy efficiency and productivity as stated in the "Conclusions on heterogeneous photocatalysis" section. Novel electrodes enabling operation at current densities close to commercially available H<sub>2</sub>O electrolyzers have to be developed. From a practical point of view, solid oxide electrodes appear to be suitable candidates. For the large-scale deployment of electrocatalytic approaches, a particular attention will be probably paid to building and managing power and heat devices. It is also expected that combining electro- or/and photocatalytic

processes with catalytic hydrogenation routes will improve the economy and even the productivity compared with the respective individual approaches.

## Acknowledgements

Dr. Chieh-Chao Yang is gratefully acknowledged for help in evaluating progress in photocatalytic CO<sub>2</sub> reduction. EVK acknowledges financial support from the Leibniz-Gemeinschaft under the research grant SAW-2011-LIKAT-2

## Notes and references

- BP, in *The BP Energy Outlook 2030*, 2013.
- <http://www.energy.alberta.ca/OilSands/1715.asp>, in *Oil Reserves in Canada*, 2012.
- B. Metz, O. Davidson, H. de Coninck, M. Loos and L. Meyer, *Carbon Dioxide Capture and Storage*, 2005.
- M. Aresta, in *Carbon Dioxide as Chemical Feedstock*, Darmstadt, 2010.
- M. Cokoja, C. Bruckmeier, B. Rieger, W. A. Herrmann and F. E. Kuhn, *Angew. Chem., Int. Ed.*, 2011, **50**, 8510.
- J. C. S. Wu, *Catal. Surv. Asia*, 2009, **13**, 30.
- G. Centi and S. Perathoner, *ChemSusChem*, 2010, **3**, 195.
- Z. Jiang, T. Xiao, V. L. Kuznetsov and P. P. Edwards, *Philos. Trans. R. Soc., A*, 2010, **368**, 3343.
- S. C. Roy, O. K. Varghese, M. Paulose and C. A. Grimes, *ACS Nano*, 2010, **4**, 1259.
- H. Takeda and O. Ishitani, *Coord. Chem. Rev.*, 2010, **254**, 346.
- J. M. Saveant, *Chem. Rev.*, 2008, **108**, 2348.
- E. E. Benson, C. P. Kubiak, A. J. Sathrum and J. M. Smieja, *Chem. Soc. Rev.*, 2009, **38**, 89.
- D. T. Whipple and P. J. A. Kenis, *J. Phys. Chem. Lett.*, 2010, **1**, 3451.
- S. N. Lvov, J. R. Beck and M. S. LaBarbera, in *Electrochemical Reduction of CO<sub>2</sub> to Fuels*, ed. N. Z. Muradov and T. Veziroglu, 2011.
- X. M. Liu, G. Q. Lu, Z. F. Yan and J. Beltramini, *Ind. Eng. Chem. Res.*, 2003, **42**, 6518.
- P. S. S. Prasad, J. W. Bae, K. W. Jun and K. W. Lee, *Catal. Surv. Asia*, 2008, **12**, 170.
- H. B. Zhang, X. L. Liang, X. Dong, H. Y. Li and G. D. Lin, *Catal. Surv. Asia*, 2009, **13**, 41.
- F. Yagi, R. Kanai, S. Wakamatsu, R. Kajiyama, Y. Suehiro and M. Shimura, *Catal. Today*, 2005, **104**, 2.
- A. J. Esswein and D. G. Nocera, *Chem. Rev.*, 2007, **107**, 4022.
- R. M. Navarro, M. A. Pena and J. L. G. Fierro, *Chem. Rev.*, 2007, **107**, 3952.
- J. D. Holladay, J. Hu, D. L. King and Y. Wang, *Catal. Today*, 2009, **139**, 244.
- R. M. Navarro, M. C. Sanchez-Sanchez, M. C. Alvarez-Galvan, F. del Valle and J. L. G. Fierro, *Energy Environ. Sci.*, 2009, **2**, 35.
- M. Curry-Nkansah, D. Driscoll, R. Farmer, R. Garland, J. Gruber, N. Gupta, F. Hershkowitz, J. Holladay, K. Nguyen, S. Schlasner, D. Steward and M. Penev, *Hydrogen Production Roadmap. Technology Pathways to the Future*, 2009.
- H. F. Abbas and W. M. A. Wan Daud, *Int. J. Hydrogen Energy*, 2010, **35**, 1160.
- P. F. v. d. Oosterkamp, in *Encyclopedia of Catalysis Synthesis Gas Generation: Industrial*, ed. I. Horvath, Weinheim, 2003.
- J. Sehested, *Catal. Today*, 2006, **111**, 103.
- J. Turner, G. Sverdrup, M. K. Mann, P.-C. Maness, B. Kroposki, M. Ghirardi, R. J. Evans and D. Blake, *Int. J. Energy Res.*, 2008, **32**, 379.
- F. E. Osterloh, *Chem. Mater.*, 2008, **20**, 35.
- A. Kudo and Y. Miseki, *Chem. Soc. Rev.*, 2009, **38**, 253.
- X. Chen, S. Shen, L. Guo and S. S. Mao, *Chem. Rev.*, 2010, **110**, 6503.
- K. Takanabe and K. Domen, *ChemCatChem*, 2012, **4**, 1485.
- D. Das, N. Khanna and T. N. Veziroglu, *Chem. Ind. Chem. Eng. Q.*, 2008, **14**, 57.
- [http://www.audi.de/de/brand/de/unternehmen/aktuelles.detail.2011-05~audi\\_balanced\\_mobility.html](http://www.audi.de/de/brand/de/unternehmen/aktuelles.detail.2011-05~audi_balanced_mobility.html), 2011.
- W. Wang, S. Wang, X. Ma and J. Gong, *Chem. Soc. Rev.*, 2011, **40**, 3703.
- T. Abe, M. Tanizawa, K. Watanabe and A. Taguchi, *Energy Environ. Sci.*, 2009, **2**, 315.
- S. Sharma, Z. Hu, P. Zhang, E. W. McFarland and H. Metiu, *J. Catal.*, 2011, **278**, 297.
- J.-N. Park and E. W. McFarland, *J. Catal.*, 2009, **266**, 92.
- F. Ocampo, B. Louis and A.-C. Roger, *Appl. Catal., A*, 2009, **369**, 90.
- G. Du, S. Lim, Y. Yang, C. Wang, L. Pfefferle and G. L. Haller, *J. Catal.*, 2007, **249**, 370.
- M. Inoue, H. Shingen, T. Kitami, S. Akamaru, A. Taguchi, Y. Kawamoto, A. Tada, K. Ohtawa, K. Ohba, M. Matsuyama, K. Watanabe, I. Tsubone and T. Abe, *J. Phys. Chem. C*, 2007, **112**, 1479.
- R. K. Thami, J. Kiwi and M. Grtzel, *Nature*, 1987, **327**, 506.
- G. Centi and S. Perathoner, *Catal. Today*, 2009, **148**, 191.
- R. W. Dorner, D. R. Hardy, F. W. Williams and H. D. Willauer, *Energy Environ. Sci.*, 2010, **3**, 884.
- Y. Q. Zhang, G. Jacobs, D. E. Sparks, M. E. Dry and B. H. Davis, *Catal. Today*, 2002, **71**, 411.
- R. W. Dorner, D. R. Hardy, F. W. Williams, B. H. Davis and H. D. Willauer, *Energy Fuels*, 2009, **23**, 4190.
- T. Herranz, S. Rojas, F. J. Prez-Alonso, M. Ojeda, P. Terreros and J. L. G. Fierro, *Appl. Catal., A*, 2006, **311**, 66.
- T. Z. Li, Y. Yang, C. H. Zhang, X. An, H. J. Wan, Z. C. Tao, H. W. Xiang, Y. W. Li, F. Yi and B. F. Xu, *Fuel*, 2007, **86**, 921.
- R. W. Dorner, D. R. Hardy, F. W. Williams and H. D. Willauer, *Appl. Catal., A*, 2010, **373**, 112.
- R. W. Dorner, D. R. Hardy, F. W. Williams and H. D. Willauer, *Catal. Commun.*, 2011, **15**, 88.
- C. Graves, S. D. Ebbesen, M. Mogensen and K. S. Lackner, *Renewable Sustainable Energy Rev.*, 2011, **15**, 1.
- G. A. Olah, A. Goepfert and G. K. S. Prakash, *Beyond Oil and Gas: The Methanol Economy*, Wiley-VCH, 2006.
- H. Goehna and P. Koenig, *CHEMTECH*, 1999, 36.
- <http://www.carbonrecycling.is/>, 2011.

- 54 F. Pontzen, W. Liebner, V. Gronemann, M. Rothaemel and B. Ahlers, *Catal. Today*, 2011, **171**, 242.
- 55 G. Liu, D. Willcox, M. Garland and H. H. Kung, *J. Catal.*, 1984, **90**, 139.
- 56 G. C. Chinchin, P. J. Denny, D. G. Parker, M. S. Spencer and D. A. Whan, *Appl. Catal.*, 1987, **30**, 333.
- 57 G. C. Chinchin, P. J. Denny, J. R. Jennings, M. S. Spencer and K. C. Waugh, *Appl. Catal.*, 1988, **36**, 1.
- 58 K. C. Waugh, *Catal. Lett.*, 2012, **142**, 1153.
- 59 X. Guo, D. Mao, G. Lu, S. Wang and G. Wu, *J. Mol. Catal. A: Chem.*, 2011, **345**, 60.
- 60 A. Bansode, B. Tidona, P. Rudolf von Rohr and A. Urakawa, *Catal. Sci. Technol.*, 2013, **3**, 767.
- 61 J. Yoshihara and C. T. Campbell, *J. Catal.*, 1996, **161**, 776.
- 62 C. V. Ovesen, B. S. Clausen, J. Schitz, P. Stoltze, H. Topsøe and J. K. Nørskov, *J. Catal.*, 1997, **168**, 133.
- 63 F. Arena, G. Italiano, K. Barbera, S. Bordiga, G. Bonura, L. Spadaro and F. Frusteri, *Appl. Catal., A*, 2008, **350**, 16.
- 64 X. Guo, D. Maob, G. Lu, S. Wang and G. Wu, *J. Catal.*, 2010, **271**, 178.
- 65 X. Guo, D. Mao, G. Lu, S. Wang and G. Wu, *Catal. Commun.*, 2011, **12**, 1095.
- 66 M. Behrens, F. Studt, I. Kasatkin, S. Kuehl, M. Haevecker, F. Abild-Pedersen, S. Zander, F. Girgsdies, P. Kurr, B.-L. Kniep, M. Tovar, R. W. Fischer, J. K. Nørskov and R. Schloegl, *Science*, 2012, **336**, 893.
- 67 E. Samei, M. Taghizadeh and M. Bahmani, *Fuel Process. Technol.*, 2012, **96**, 128.
- 68 P. Gao, F. Li, F. Xiao, N. Zhao, N. Sun, W. Wei, L. Zhong and Y. Sun, *Catal. Sci. Technol.*, 2012, **2**, 1447.
- 69 L. Zhang, Y. Zhang and S. Chen, *Appl. Catal., A*, 2012, **415–416**, 118.
- 70 K. T. Jung and A. T. Bell, *Catal. Lett.*, 2002, **80**, 63.
- 71 F. Liao, Y. Huang, J. Ge, W. Zheng, K. Tedsree, P. Collier, X. Hong and S. C. Tsang, *Angew. Chem., Int. Ed.*, 2011, **50**, 2162.
- 72 X.-L. Liang, X. Dong, G.-D. Lin and H.-B. Zhang, *Appl. Catal., B*, 2009, **88**, 315.
- 73 H. Kong, H. Y. Li, G. D. Lin and H. B. Zhang, *Catal. Lett.*, 2011, **141**, 886.
- 74 V. M. Lebarbier, R. A. Dagle, L. Kovarik, J. A. Lizarazo-Adarme, D. L. King and D. R. Palo, *Catal. Sci. Technol.*, 2012, **2**, 2116.
- 75 N. Koizumi, X. Jiang, J. Kugai and C. Song, *Catal. Today*, 2012, **194**, 16.
- 76 X. Zhou, J. Qu, F. Xu, J. Hu, J. S. Foord, Z. Zeng, X. Hong and S. C. E. Tsang, *Chem. Commun.*, 2013, **49**, 1747.
- 77 A. B. Vidal, L. Fera, J. Evans, Y. Takahashi, P. Liu, K. Nakamura, F. Illas and J. A. Rodriguez, *J. Phys. Chem. Lett.*, 2012, **3**, 2275.
- 78 Y. F. Zhao, Y. Yang, C. Mims, C. H. F. Peden, J. Li and D. Mei, *J. Catal.*, 2011, **281**, 199.
- 79 L. C. Grabow and M. Mavrikakis, *ACS Catal.*, 2011, **1**, 365.
- 80 M. Gattrell, N. Gupta and A. Co, *J. Electroanal. Chem.*, 2006, **594**, 1.
- 81 D. L. DuBois, in *Electrochemical Reactions of Carbon Dioxide*, ed. A. J. Bard, M. Stratmann, F. Scholz and C. J. Pickett, Weinheim, 2006.
- 82 M. R. DuBois and D. L. DuBois, *Acc. Chem. Res.*, 2009, **42**, 1974.
- 83 K. Hori, in *Handbook of Fuels Cells CO<sub>2</sub>-Reduction, Catalyzed by Metal Electrodes*, 2010.
- 84 C. Costentin, M. Robert and J.-M. Saveant, *Chem. Soc. Rev.*, 2013, **42**, 2423.
- 85 Y. Hori, A. Murata and R. Takahashi, *J. Chem. Soc., Faraday Trans. 1*, 1989, **85**, 2309.
- 86 Y. Hori, H. Wakebe, T. Tsukamoto and O. Koga, *Electrochim. Acta*, 1994, **39**, 1833.
- 87 M. Watanabe, M. Shibata, A. Katoh, M. Azuma and T. Sakata, *Denki Kagaku*, 1991, **59**, 508.
- 88 R. L. Cook, R. C. MacDuff and A. F. Sammells, *J. Electrochem. Soc.*, 1988, **135**, 1320.
- 89 Y. Hori, I. Takahashi, O. Koga and N. Hoshi, *J. Mol. Catal. A: Chem.*, 2003, **199**, 39.
- 90 M. N. Mahmood, D. Masheder and C. J. Harty, *J. Appl. Electrochem.*, 1987, **17**, 1159.
- 91 K. Hara, A. Kudo, T. Sakata and M. Watanabe, *J. Electrochem. Soc.*, 1995, **142**, L57.
- 92 T. Kobayashi and H. Takahashi, *Energy Fuels*, 2003, **18**, 285.
- 93 Y. Kohno, T. Yamamoto, T. Tanaka and T. Funabiki, *J. Mol. Catal. A: Chem.*, 2001, **175**, 173.
- 94 C. Delacourt, P. L. Ridgway, J. B. Kerr and J. Newman, *J. Electrochem. Soc.*, 2008, **155**, B42.
- 95 E. Dufek, T. Lister and M. McIlwain, *J. Appl. Electrochem.*, 2011, **41**, 623.
- 96 E. J. Dufek, T. E. Lister, S. G. Stone and M. E. McIlwain, *J. Electrochem. Soc.*, 2012, **159**, F514.
- 97 S. R. Narayanan, B. Haines, J. Soler and T. I. Valdez, *J. Electrochem. Soc.*, 2011, **158**, A167.
- 98 E. E. Barton, D. M. Rampulla and A. B. Bocarsly, *J. Am. Chem. Soc.*, 2008, **130**, 6342.
- 99 B. A. Rosen, A. Salehi-Khojin, M. R. Thorson, W. Zhu, D. T. Whipple, P. J. A. Kenis and R. I. Masel, *Science*, 2011, **334**, 643.
- 100 M. R. Goncalves, A. Gomes, J. Condeco, R. Fernandes, T. Pardal, C. A. C. Sequeira and J. B. Branco, *Energy Convers. Manage.*, 2010, **51**, 30.
- 101 M. Le, M. Ren, Z. Zhang, P. T. Sprunger, R. L. Kurtz and J. C. Flake, *J. Electrochem. Soc.*, 2011, **158**, E45.
- 102 C. W. Li and M. W. Kanan, *J. Am. Chem. Soc.*, 2012, **134**, 7231.
- 103 Y. Chen and M. W. Kanan, *J. Am. Chem. Soc.*, 2012, **134**, 1986.
- 104 Z. Chen, P. Kang, M.-T. Zhang, B. R. Stoner and T. J. Meyer, *Energy Environ. Sci.*, 2013, **6**, 813.
- 105 C. M. Stoots, J. E. O'Brien, J. S. Herring and J. J. Hartvigsen, *J. Fuel Cell Sci. Technol.*, 2009, **6**, 011014.
- 106 Z. Zhan, W. Kobsiriphat, J. R. Wilson, M. Pillai, I. Kim and S. A. Barnett, *Energy Fuels*, 2009, **23**, 3089.
- 107 S. D. Ebbesen, C. Graves and M. Mogensen, *Int. J. Green Energy*, 2009, **6**, 646.

- 108 B. Hu, V. Stancovski, M. Morton and S. L. Suib, *Appl. Catal., A*, 2010, **382**, 277.
- 109 C. Graves, S. D. Ebbesen and M. Mogensen, *Solid State Ionics*, 2011, **192**, 398.
- 110 K. Xie, Y. Zhang, G. Meng and J. T. S. Irvine, *J. Mater. Chem.*, 2011, **21**, 195.
- 111 Z. Zhan and L. Zhao, *J. Power Sources*, 2010, **195**, 7250.
- 112 E. E. Barton, D. M. Rampulla and A. B. Bocarsly, *J. Am. Chem. Soc.*, 2008, **130**, 6342.
- 113 A. J. Morris, R. T. McGibbon and A. B. Bocarsly, *ChemSusChem*, 2011, **4**, 191.
- 114 S. Cheng, D. Xing, D. F. Call and B. E. Logan, *Environ. Sci. Technol.*, 2009, **43**, 3953.
- 115 M. Villano, F. Aulenta, C. Ciucci, T. Ferri, A. Giuliano and M. Majone, *Bioresour. Technol.*, 2010, **101**, 3085.
- 116 H. Zhao, Y. Zhang, B. Zhao, Y. Chang and Z. Li, *Environ. Sci. Technol.*, 2012, **46**, 5198.
- 117 M. C. A. A. Van Eerten-Jansen, A. Ter Heijne, C. J. N. Buisman and H. V. M. Hamelers, *Int. J. Energy Res.*, 2012, **36**, 809.
- 118 T. Mogi, T. Ishii, K. Hashimoto and R. Nakamura, *Chem. Commun.*, 2013, **49**, 3967.
- 119 H. Li, P. H. Opgenorth, D. G. Wernick, S. Rogers, T.-Y. Wu, W. Higashide, P. Malati, Y.-X. Huo, K. M. Cho and J. C. Liao, *Science*, 2012, **335**, 1596.
- 120 V. Augugliaro, L. Palmisano and M. Schiavello, *AIChE J.*, 1991, **37**, 1096.
- 121 M. Salaices, B. Serrano and H. I. de Lasa, *Chem. Eng. J.*, 2002, **90**, 219.
- 122 O. M. Alfano, M. I. Cabrera and A. E. Cassano, *Chem. Eng. Sci.*, 1994, **49**, 5327.
- 123 G. Mul, C. Schacht, W. P. M. van Swaaij and J. A. Moulijn, *Chem. Eng. Process.*, 2012, **51**, 137.
- 124 P. Pathak, M. J. Meziani, L. Castillo and Y. P. Sun, *Green Chem.*, 2005, **7**, 667.
- 125 C.-C. Yang, J. Vernimmen, V. Meynen, P. Cool and G. Mul, *J. Catal.*, 2011, **284**, 1.
- 126 J. C. S. Wu, H. M. Lin and C. L. Lai, *Appl. Catal., A*, 2005, **296**, 194.
- 127 Z. Y. Wang, H. C. Chou, J. C. S. Wu, D. P. Tsai and G. Mul, *Appl. Catal., A*, 2010, **380**, 172.
- 128 M. Halmann, *Nature*, 1978, **275**, 115.
- 129 T. Inoue, A. Fujishima, S. Konishi and K. Honda, *Nature*, 1979, **277**, 637.
- 130 K. R. Thampi, J. Kiwi and M. Gratzel, *Nature*, 1987, **327**, 506.
- 131 K. Hirano, K. Inoue and T. Yatsu, *J. Photochem. Photobiol., A*, 1992, **64**, 255.
- 132 O. Ishitani, C. Inoue, Y. Suzuki and T. Ibusuki, *J. Photochem. Photobiol., A*, 1993, **72**, 269.
- 133 M. Anpo, H. Yamashita, Y. Ichihashi and S. Ehara, *J. Electroanal. Chem.*, 1995, **396**, 21.
- 134 H. Yamashita, A. Shiga, S. Kawasaki, Y. Ichihashi, S. Ehara and M. Anpo, *Energy Convers. Manage.*, 1995, **36**, 617.
- 135 F. Saladin, L. Forss and I. Kamber, *J. Chem. Soc., Chem. Commun.*, 1995, 533.
- 136 F. Saladin and I. Alxneit, *J. Chem. Soc., Faraday Trans.*, 1997, **93**, 4159.
- 137 S. Kaneco, Y. Shimizu, K. Ohta and T. Mizuno, *J. Photochem. Photobiol., A*, 1998, **115**, 223.
- 138 H. Yamashita, Y. Fujii, Y. Ichihashi, S. G. Zhang, K. Ikeue, D. R. Park, K. Koyano, T. Tatsumi and M. Anpo, *Catal. Today*, 1998, **45**, 221.
- 139 M. Subrahmanyam, S. Kaneco and N. Alonso-Vante, *Appl. Catal., B*, 1999, **23**, 169.
- 140 K. Ikeue, H. Mukai, H. Yamashita, S. Inagaki, M. Matsuoka and M. Anpo, *J. Synchrotron Radiat.*, 2001, **8**, 640.
- 141 K. Ikeue, H. Yamashita, M. Anpo and T. Takewaki, *J. Phys. Chem. B*, 2001, **105**, 8350.
- 142 I. H. Tseng, W. C. Chang and J. C. S. Wu, *Appl. Catal., B*, 2002, **37**, 37.
- 143 I. Keita, S. Nozaki, M. Ogawa and M. Anpo, *Catal. Today*, 2002, **74**, 241.
- 144 G. Q. Guan, T. Kida and A. Yoshida, *Appl. Catal., B*, 2003, **41**, 387.
- 145 G. R. Dey, A. D. Belapurkar and K. Kishore, *J. Photochem. Photobiol., A*, 2004, **163**, 503.
- 146 I. H. Tseng and J. C. S. Wu, *Catal. Today*, 2004, **97**, 113.
- 147 I. H. Tseng, J. C. S. Wu and H. Y. Chou, *J. Catal.*, 2004, **221**, 432.
- 148 Y. Ku, W. H. Lee and W. Y. Wang, *J. Mol. Catal. A: Chem.*, 2004, **212**, 191.
- 149 J. S. Hwang, J. S. Chang, S. E. Park, K. Ikeue and M. Anpo, *Top. Catal.*, 2005, **35**, 311.
- 150 N. Sasirekha, S. J. S. Basha and K. Shanthi, *Appl. Catal., B*, 2006, **62**, 169.
- 151 S. S. Tan, L. Zou and E. Hu, *Sci. Technol. Adv. Mater.*, 2007, **8**, 89.
- 152 X. H. Xia, Z. H. Jia, Y. Yu, Y. Liang, Z. Wang and L. L. Ma, *Carbon*, 2007, **45**, 717.
- 153 S. H. Liu, Z. H. Zhao and Z. Z. Wang, *Photochem. Photobiol. Sci.*, 2007, **6**, 695.
- 154 P. W. Pan and Y. W. Chen, *Catal. Commun.*, 2007, **8**, 1546.
- 155 G. H. Li, S. Ciston, Z. V. Saponjic, L. Chen, N. M. Dimitrijevic, T. Rajh and K. A. Gray, *J. Catal.*, 2008, **253**, 105.
- 156 T. V. Nguyen and J. C. S. Wu, *Appl. Catal., A*, 2008, **335**, 112.
- 157 O. K. Varghese, M. Paulose, T. J. LaTempa and C. A. Grimes, *Nano Lett.*, 2009, **9**, 731.
- 158 H. C. Yang, H. Y. Lin, Y. S. Chien, J. C. S. Wu and H. H. Wu, *Catal. Lett.*, 2009, **131**, 381.
- 159 Q. H. Zhang, W. D. Han, Y. J. Hong and J. G. Yu, *Catal. Today*, 2009, **148**, 335.
- 160 H. Tsuneoka, K. Teramura, T. Shishido and T. Tanaka, *J. Phys. Chem. C*, 2010, **114**, 8892.
- 161 K. Koci, K. Mateju, L. Obalova, S. Krejciikova, Z. Lacny, D. Placha, L. Capek, A. Hospodkova and O. Solcova, *Appl. Catal., B*, 2010, **96**, 239.
- 162 Y. Li, W. N. Wang, Z. L. Zhan, M. H. Woo, C. Y. Wu and P. Biswas, *Appl. Catal., B*, 2010, **100**, 386.
- 163 Q. Liu, Y. Zhou, J. H. Kou, X. Y. Chen, Z. P. Tian, J. Gao, S. C. Yan and Z. G. Zou, *J. Am. Chem. Soc.*, 2010, **132**, 14385.
- 164 S. C. Yan, S. X. Ouyang, J. Gao, M. Yang, J. Y. Feng, X. X. Fan, L. J. Wan, Z. S. Li, J. H. Ye, Y. Zhou and Z. G. Zou, *Angew. Chem., Int. Ed.*, 2010, **49**, 6400.

- 165 C. J. Wang, R. L. Thompson, J. Baltrus and C. Matranga, *J. Phys. Chem. Lett.*, 2010, **1**, 48.
- 166 K. Kočí, V. Matějka, P. Kovář, Z. Lacný and L. Obalová, *Catal. Today*, 2011, **161**, 105.
- 167 Q. Zhang, T. Gao, J. M. Andino and Y. Li, *Appl. Catal., B*, 2012, **123–124**, 257.
- 168 P.-Q. Wang, Y. Bai, J.-Y. Liu, Z. Fan and Y.-Q. Hu, *Catal. Commun.*, 2012, **29**, 185.
- 169 W.-H. Lee, C.-H. Liao, M.-F. Tsai, C.-W. Huang and J. C. S. Wu, *Appl. Catal., B*, 2013, **132–133**, 445.
- 170 Y. Wang, B. Li, C. Zhang, L. Cui, S. Kang, X. Li and L. Zhou, *Appl. Catal., B*, 2013, **130–131**, 277.
- 171 A. Dhakshinamoorthy, S. Navalon, A. Corma and H. Garcia, *Energy Environ. Sci.*, 2012, **5**, 9217.
- 172 K. Ikeue, H. Yamashita, M. Anpo and T. Takewaki, *J. Phys. Chem. B*, 2001, **105**, 8350.
- 173 T. Maschmeyer and M. Che, *Angew. Chem., Int. Ed.*, 2010, **49**, 1536.
- 174 T. Maschmeyer and M. Che, *Angew. Chem., Int. Ed.*, 2010, **49**, 9590.
- 175 C. C. Yang, Y. H. Yu, B. van der Linden, J. C. S. Wu and G. Mul, *J. Am. Chem. Soc.*, 2010, **132**, 8398.
- 176 H. Frei, *Chimia*, 2009, **63**, 721.
- 177 W. Y. Lin and H. Frei, *Cron. Chim.*, 2006, **9**, 207.
- 178 W. Y. Lin, H. X. Han and H. Frei, *J. Phys. Chem. B*, 2004, **108**, 18269.
- 179 N. Ulagappan and H. Frei, *J. Phys. Chem. A*, 2000, **104**, 7834.
- 180 N. Sivasankar, W. W. Weare and H. Frei, *J. Am. Chem. Soc.*, 2011, **133**, 12976.
- 181 F. Jiao and H. Frei, *Energy Environ. Sci.*, 2010, **3**, 1018.
- 182 F. E. Osterloh, *Chem. Soc. Rev.*, 2013, **42**, 2294.
- 183 T. Wang, L. Yang, X. Du and Y. Yang, *Energy Convers. Manage.*, 2013, **65**, 299.
- 184 K. Chandrasekaran and J. K. Thomas, *Chem. Phys. Lett.*, 1983, **99**, 7.
- 185 M. W. Raphael and M. A. Malati, *J. Photochem. Photobiol., A*, 1989, **46**, 367.
- 186 M. A. Malati, L. Attubato and K. Beaney, *Sol. Energy Mater.*, 1996, **40**, 1.
- 187 N. M. Dimitrijevic, B. K. Vijayan, O. G. Poluektov, T. Rajh, K. A. Gray, H. Y. He and P. Zapol, *J. Am. Chem. Soc.*, 2011, **133**, 3964.
- 188 T. Ohno, K. Sarukawa and M. Matsumura, *New J. Chem.*, 2002, **26**, 1167.
- 189 Y. Zheng, J. Liu, J. Liang, M. Jaroniec and S. Z. Qiao, *Energy Environ. Sci.*, 2012, **5**, 6717.
- 190 H. S. Soo, A. Agiral, A. Bachmeier and H. Frei, *J. Am. Chem. Soc.*, 2012, **134**, 17104.
- 191 F. Neese, *Coord. Chem. Rev.*, 2009, **253**, 526.
- 192 C. J. Cramer and D. G. Truhlar, *Phys. Chem. Chem. Phys.*, 2009, **11**, 10757.
- 193 P. Gori-Giorgi and M. Seidl, *Phys. Chem. Chem. Phys.*, 2010, **12**, 14405.
- 194 K. Burke, *J. Chem. Phys.*, 2012, **136**, 150901.
- 195 A. J. Cohen, P. Mori-Sánchez and W. Yang, *Chem. Rev.*, 2012, **112**, 289.
- 196 C. R. Jacob and M. Reiher, *arXiv.org, e-Print Arch., Phys.*, 2012, **1**.
- 197 R. Zhang, H. Liu, B. Wang and L. Ling, *Appl. Catal., B*, 2012, **126**, 108.
- 198 R. Zhang, B. Wang, H. Liu and L. Ling, *J. Phys. Chem. C*, 2011, **115**, 19811.
- 199 S. Yin, T. Swift and Q. Ge, *Catal. Today*, 2011, **165**, 10.
- 200 S. Yin and Q. Ge, *Catal. Today*, 2012, **194**, 30.
- 201 S.-Y. Wu and J.-J. Ho, *J. Phys. Chem. C*, 2012, **116**, 13202.
- 202 P. Liu, Y. Choi, Y. Yang and M. G. White, *J. Phys. Chem. A*, 2009, **114**, 3888.
- 203 G. R. Jackson and D. Mahajan, in Method for production of mixed alcohols from synthesis gas, *US Pat.*, 6,248,796, 2011.
- 204 S. Yin, Z. Wang and E. R. Bernstein, *Phys. Chem. Chem. Phys.*, 2013, **15**, 4699.
- 205 A. A. Peterson, F. Abild-Pedersen, F. Studt, J. Rossmeisl and J. K. Nørskov, *Energy Environ. Sci.*, 2010, **3**, 1311.
- 206 W. J. Durand, A. A. Peterson, F. Studt, F. Abild-Pedersen and J. K. Nørskov, *Surf. Sci.*, 2011, **605**, 1354.
- 207 A. A. Peterson and J. K. Nørskov, *J. Phys. Chem. Lett.*, 2012, **3**, 251.
- 208 J. A. Keith and E. A. Carter, *J. Am. Chem. Soc.*, 2012, **134**, 7580.
- 209 C. E. Barton, P. S. Lakkaraju, D. M. Rampulla, A. J. Morris, E. Abelev and A. B. Bocarsly, *J. Am. Chem. Soc.*, 2010, **132**, 11539.
- 210 M. Z. Kamrath, R. A. Relph and M. A. Johnson, *J. Am. Chem. Soc.*, 2010, **132**, 15508.
- 211 A. J. Morris, R. T. McGibbon and A. B. Bocarsly, *ChemSusChem*, 2011, **4**, 191.
- 212 J. A. Keith and E. A. Carter, *J. Chem. Theory Comput.*, 2012, **8**, 8187.
- 213 K. Xie, N. Umezawa, N. Zhang, P. Reunchan, Y. Zhang and J. Ye, *Energy Environ. Sci.*, 2011, **4**, 4211.
- 214 S. Luo, Y. Zhao and D. G. Truhlar, *J. Phys. Chem. Lett.*, 2012, **3**, 2975.
- 215 H. Shi and Z. Zou, *J. Phys. Chem. Solids*, 2012, **73**, 788.
- 216 M. C. Toroker, D. K. Kanan, N. Alidoust, L. Y. Isseroff, P.-L. Liao and E. A. Carter, *Phys. Chem. Chem. Phys.*, 2011, **13**, 16644.
- 217 P. Li, S. Ouyang, G. Xi, T. Kako and J. Ye, *J. Phys. Chem. C*, 2012, **116**, 7621.
- 218 F. Alharbi, J. D. Bass, A. Salhi, A. Alyamani, H.-C. Kim and R. D. Miller, *Renewable Energy*, 2011, **36**, 2753.
- 219 H. Li, Y. Lei, Y. Huang, Y. Fang, Y. Xu, L. Zhu and X. Li, *J. Nat. Gas Chem.*, 2011, **20**, 145.
- 220 R. D. Richardson, E. J. Holland and B. K. Carpenter, *Nat. Chem.*, 2011, **3**, 301.
- 221 B. K. Carpenter and I. Rose, *ARKIVOC*, 2012, 127.
- 222 L. Gonzalez, D. Escudero and L. Serrano-Andrés, *ChemPhysChem*, 2012, **13**, 28.
- 223 J. Baltrusaitis, E. V. Patterson and C. Hatch, *J. Phys. Chem. A*, 2012, **116**, 9331.
- 224 R. F. Höckendorf, C.-K. Siu, C. van der Linde, O. P. Balaj and M. K. Beyer, *Angew. Chem., Int. Ed.*, 2010, **49**, 8257.
- 225 A. Jess, P. Kaiser, C. Kern, R. B. Unde and C. von Olshausen, *Chem. Ing. Tech.*, 2011, **83**, 1777.
- 226 <http://www.mantraenergy.com/Technology/ERCTechnology.aspx>.